

# Lawrence Berkeley National Laboratory

## Lawrence Berkeley National Laboratory

### **Title**

A Korarchael Genome Reveals Insights into the Evolution of the Archaea

### **Permalink**

<https://escholarship.org/uc/item/28w1d3zs>

### **Author**

Elkins, James G.

### **Publication Date**

2008-09-03

## A korarchaeal genome reveals insights into the evolution of the Archaea

James G. Elkins<sup>\*†</sup>, Mircea Podar<sup>‡</sup>, David E. Graham<sup>§</sup>, Kira S. Makarova<sup>¶</sup>, Yuri Wolf<sup>¶</sup>, Lennart Randau<sup>||</sup>, Brian P. Hedlund<sup>\*\*</sup>, Céline Brochier-Armanet<sup>††</sup>, Victor Kunin<sup>‡‡</sup>, Iain Anderson<sup>‡‡</sup>, Alla Lapidus<sup>‡‡</sup>, Eugene Goltsman<sup>‡‡</sup>, Kerrie Barry<sup>‡‡</sup>, Eugene V. Koonin<sup>¶</sup>, Phil Hugenholtz<sup>‡‡</sup>, Nikos Kyrpides<sup>‡‡</sup>, Gerhard Wanner<sup>§§</sup>, Paul Richardson<sup>‡‡</sup>, Martin Keller<sup>‡</sup>, and Karl O. Stetter<sup>\*¶|||</sup>

<sup>\*</sup>Lehrstuhl für Mikrobiologie und Archaeenzentrum, Universität Regensburg, D-93053, Regensburg, Germany; <sup>‡</sup>Biosciences Division, Oak Ridge National Laboratory, Oak Ridge, TN 37831; <sup>§</sup>Department of Chemistry and Biochemistry, The University of Texas at Austin, Austin, TX 78712; <sup>¶</sup>National Center for Biotechnology Information, National Library of Medicine, National Institutes of Health, Bethesda, MD 20894; <sup>||</sup>Department of Molecular Biophysics and Biochemistry, Yale University, New Haven, CT 06520; <sup>\*\*</sup>School of Life Sciences, University of Nevada, Las Vegas, NV, 89154; <sup>††</sup>Université de Provence - Aix-Marseille I, Laboratoire de chimie bactérienne, UPR CNRS 9043, Marseille, France; <sup>‡‡</sup>DOE Joint Genome Institute, Walnut Creek, CA 94598; <sup>§§</sup>Institute of Botany, LM University of Munich, D-80638, Munich, Germany; <sup>¶¶</sup>Institute of Geophysics and Planetary Science, University of California, Los Angeles, CA 90095

<sup>†</sup>Present address: Biosciences Division, Oak Ridge National Laboratory, Oak Ridge, TN 37831

<sup>|||</sup>To whom correspondence should be addressed:

Karl O. Stetter  
Universität Regensburg  
Lehrstuhl für Mikrobiologie  
Universitätstraße 31  
93343 Regensburg  
Phone: +49-941 943-1821, -3161  
Fax: +49-941 943-3243  
E-Mail: [karl.stetter@biologie.uni-regensburg.de](mailto:karl.stetter@biologie.uni-regensburg.de)

Manuscript info: 13 pages, 2 figures, 2 tables.

Abbreviations: SSU, small subunit; LSU, large subunit; arCOGs, archaeal clusters of orthologous groups; RNAP, RNA polymerase; EF, elongation factor; HGT, horizontal gene transfer.

The genome sequence describe here has been deposited in GenBank under accession no. CP000968.

**Abstract:**

The candidate division *Korarchaeota* comprises a group of uncultivated microorganisms which, by their small subunit rRNA phylogeny, may have diverged early from the major archaeal phyla *Crenarchaeota* and *Euryarchaeota*. Here we report the initial characterization of a member of the *Korarchaeota* with the proposed name, “*Candidatus Korarchaeum cryptofilum*” which exhibits an ultra-thin, filamentous morphology. To investigate possible ancestral relationships between deep-branching *Korarchaeota* and other phyla, we used whole-genome shotgun (WGS) sequencing to construct a complete, composite korarchaeal genome from enriched cells. The genome was assembled into a single contig 1.59 Mb in length with a G+C content of 49%. Of the 1617 predicted protein-coding genes, 1382 (85%) could be assigned to a revised set of archaeal COGs. The predicted gene functions suggest that the organism relies on a simple mode of peptide fermentation for carbon and energy and lacks the ability to synthesize *de novo* purines, coenzyme A, and several other cofactors. Phylogenetic analyses based on conserved single genes and concatenated protein sequences positioned the korarchaeote as a deep archaeal lineage with an apparent affinity to the *Crenarchaeota*. However, the predicted gene content revealed that several conserved cellular systems such as cell division, DNA replication, and tRNA maturation resemble the counterparts in the *Euryarchaeota*. In light of the known composition of archaeal genomes, the *Korarchaeota* might have retained a set of cellular features that represents the ancestral archaeal form.

**Introduction:**

Two established phyla, the *Crenarchaeota* and *Euryarchaeota*, divide the archaeal domain based on fundamental differences in translation, transcription and replication (1). Yet hydrothermal environments have yielded small subunit (SSU) rRNA gene sequences that form deep-branching phylogenetic lineages, which potentially lie outside of these major groups. These uncultivated organisms include members of the *Korarchaeota* (2-4), the Ancient Archaeal Group (5), and the Marine Hydrothermal Vent Group (5, 6). The Nanoarchaeota have also been suggested to hold a basal phylogenetic position (7) but this placement has been debated (8). The *Korarchaeota* comprise the largest group of deep-branching, unclassified archaea and have been detected in several geographically isolated terrestrial and marine thermal environments (2, 4, 5, 9-17).

To gain new insights into the *Korarchaeota*, we revisited the original site where Barns et al. (2) collected the first korarchaeal environmental SSU rDNA sequences (pJP78 and pJP27) from Obsidian Pool, Yellowstone National Park, Wyoming, USA. Continuous enrichment cultures were established at 85° C using a dilute organic medium and sediment samples from Obsidian Pool as an inoculum. The cultivation system supported the stable growth of a mixed community of hyperthermophilic bacteria and archaea including an organism with a SSU rDNA sequence displaying 99% identity to pJP27. The organism was identified as an ultra-thin filament between 0.16-0.18  $\mu\text{m}$  in diameter and variable in length. Whole-genome shotgun (WGS) sequencing was used to assemble an intact composite genome from purified cells originating from the enrichment culture. The complete genome sequence of “*Candidatus (Ca.) Korarchaeum cryptofilum*” provides the first look into the biology of these deeply-branching archaea and their evolutionary relationships with *Crenarchaeota* and *Euryarchaeota*.

## Results:

**Cultivation and *In-situ* Identification.** An enrichment culture was inoculated with sediment and hot spring samples taken from Obsidian Pool, YNP. The enrichment was maintained under strictly anaerobic conditions at 85° C, pH 6.5 and continuously fed a dilute organic medium. A stable community of hyperthermophilic archaea and bacteria with a total cell density of approx.  $1.0 \times 10^8$  cells/ml was supported for nearly 4 years. Sequences from SSU rDNA clone libraries derived from the enrichment were closely related to other known isolates or environmental sequences from Obsidian Pool [see supporting information (SI) *Text* and SI Fig. 3]. The *Korarchaeota*, were represented by the SSU rDNA clone pOPF\_08 which is 99% identical to pJP27 from Obsidian Pool, YNP (2), and pAB5 from Calcite Springs, YNP (9). FISH analysis allowed the positive identification of cells with the pOPF\_08 SSU rRNA sequence. Cells hybridizing to Cy3-labeled, *Korarchaeota*-specific probes, KR515R and KR565R, were ultra-thin filaments less than 0.2  $\mu\text{m}$  in diameter with an average length of 15  $\mu\text{m}$ , although cells were observed with lengths up to 100  $\mu\text{m}$  (Fig. 1A, SI Fig. 4, SI *Text*).

**Cell Preparation and Genome Sequencing.** It was observed that filamentous cells hybridizing to probes KR515R/KR565R remained intact in the presence of high concentrations of sodium dodecyl sulphate (SDS; up to 1%) in the hybridization buffer. This feature allowed highly enriched cell preparations to be made by exposing the Obsidian Pool enrichment culture to 0.2% (w/v) SDS (without cell fixation) followed by several washing steps and filtration through 0.45  $\mu\text{m}$  syringe filters. PCR amplified, SSU rDNA sequences from SDS-treated, filtered cell preparations showed that over 99% of the clones sequenced ( $n=180$ ) were identical to the SSU rDNA sequence of pOPF\_08 (See SI Fig. 5). Phase contrast (Fig. 1B) and electron microscopy (Fig. 1C) showed the samples to be highly enriched for ultra-thin filamentous cells with a diameter of 0.16-0.18  $\mu\text{m}$ . DNA clone libraries were constructed from both SDS and non-SDS (libraries BHXI and BFPP respectively) treated enrichment culture filtrates. A total of 23,000 and 11,520 quality sequencing reads from libraries BHXI and BFPP respectively were binned based on %GC content and read depth. Overlapping fosmid sequences containing the pOPF\_08 SSU rRNA gene (SI Fig. 6) were used to guide the WGS assembly. Five large scaffolds with a read depth of 8.4-9.9X were closed by PCR (further details are provided in SI *Text*). Single nucleotide polymorphisms occur at a rate of approx. 0.2% across the genome.

**General Features.** The complete genome consists of a circular chromosome 1,590,757 bp in length with an average G+C content of 49% (Table 1). A single operon was identified that contains genes for the SSU and LSU rRNAs. Forty five tRNAs were identified using tRNAscan-SE (18). A total of 1617 protein coding genes were predicted with an average size of 870 bp. Of the predicted protein coding genes, 72.4% included AUG; 17.6%, UUG; and 10% had GUG for start codons. The arCOG (see below) and COG analysis, combined with additional database searches allowed the assignment of a specific biological function to 998 (62%) predicted proteins; for another 246 proteins (15%), biochemical activity but not biological function could be predicted, and for the remaining 373 (23%) proteins, no functional prediction was possible, although many of these are conserved in some other archaea and/or bacteria.

**Archaeal COGs.** The predicted proteins were assigned to archaeal COGs [(arCOGs) (19) (see SI *Text*, SI Table 3)]. Of the 1617 annotated proteins, 1382 (85%) were found to belong to the

arCOGs, a coverage that is slightly lower than the mean coverage of 88% for other archaea and much greater than the lowest coverage obtained for *Nanoarchaeum equitans* (72%) and *Cenarchaeum symbiosum* (58%). When the gene complement was compared to the strictly defined core gene sets for the *Euryarchaeota* and *Crenarchaeota* (i.e., genes that are represented in all sequenced genomes from the respective division, with the possible exception for *C. symbiosum* in the case of the *Crenarchaeota*, but are missing in at least some organisms of the other division), a strong affinity with the *Crenarchaeota* was readily apparent. Specifically, “*Ca. K. cryptofilum*” possesses 169 of the 201 genes from the crenarchaeal core (84%) but only 33 of the 52 genes from the euryarchaeal core (63%). When the core gene sets were defined more liberally, i.e., as genes that are present in more than two thirds of the genomes from one division and absent in the other division, the korarchaeote actually shared more genes with the *Euryarchaeota* than with *Crenarchaeota* (Table 2, SI Table 4). Seven proteins had readily identifiable bacterial but not archaeal orthologs, as determined by assigning proteins to bacterial COGs (20) (SI Table 5). Conceivably, the respective genes were captured via independent horizontal gene transfer (HGT) events from various bacteria. By contrast, there were no proteins specifically shared with eukaryotes, to the exclusion of other archaea. The organism lacks only 5 genes that are represented in all sequenced archaeal genomes, namely, diphthamide synthase subunit DPH2, diphthamide biosynthesis methyltransferase, predicted ATPase of PP-loop superfamily; predicted Zn-ribbon RNA-binding protein, and small-conductance mechanosensitive channel.

**Energy Metabolism.** The predicted gene set suggests that “*Ca. K. cryptofilum*” grows heterotrophically, using a variety of peptide and amino acid degradation pathways. At least four ABC-type oligopeptide transporters and an OPT-type symporter could import short peptides, which more than a dozen peptidases could hydrolyze into amino acids. As in *Pyrococcus* spp., pyridoxal 5'-phosphate dependent aminotransferases can convert amino acids to 2-oxoacids, while scavenging amines with  $\alpha$ -keto-glutarate to form glutamate. Four ferredoxin-dependent oxidoreductases (specific for indolepyruvate, pyruvate, 2-oxoglutarate or 2-oxoisovalerate) could oxidize and decarboxylate the 2-oxoacids, producing acyl-CoA molecules. Four acyl-CoA synthetases can convert this thioester bond energy into phosphoanhydride equivalents. Six aldehyde:ferredoxin oxidoreductase metalloenzymes could oxidize aldehydes derived from these amino acids. Pyruvate could be degraded by this pathway or by a homolog of pyruvate formate lyase. The only terminal reduction reaction predicted from the genome sequence is hydrogen production, apparently catalyzed by two soluble [NiFe]-hydrogenases. An archaeal-type proton-transporting ATP synthase would convert proton motive force produced by anaerobic respiration into ATP. However, in contrast to the system proposed for *Pyrococcus furiosus*, “*Ca. K. cryptofilum*” lacks a membrane-bound proton-translocating hydrogenase (21). Therefore proton translocation must occur through the NADH:quinone oxidoreductase complex or a novel system that might involve homologs of the methanogen *hdrABC*-type heterodisulfide reductase complex. A ferredoxin:NADP oxidoreductase, three flavin reductases, and two electron transfer flavoproteins could mediate electron transfer to the respiratory chain. The korarchaeote also encodes a homolog of a single subunit [Ni-Fe] carbon monoxide dehydrogenase and its accessory proteins in a cluster of methanogen-like genes. Although the physiological role of these proteins in methanogens is unknown, they might confer the ability to oxidize CO produced under anaerobic conditions (22). There is no cytochrome c and no evidence of the dissimilatory reduction of sulfur, sulfite, sulfate, nitrate, nitrite, iron, formate, or oxygen. An abundance of

iron-sulfur proteins, free radical initiating enzymes and the lack of oxidases suggest a strictly anaerobic lifestyle.

**Central Metabolism.** A partial citric acid cycle is present which includes 2-oxoglutarate: ferredoxin oxidoreductase, succinyl-CoA ligase, succinate dehydrogenase, fumarase, malate dehydrogenase, aconitase, and malic enzyme. These enzymes could be used either for the degradation or for the biosynthesis of glutamate. The organism also encodes the components of a serine hydroxymethyltransferase and glycine cleavage system. One-carbon units from this pterin-dependent pathway are used to produce methionine from homocysteine. The genome encodes few carbohydrate transporters and no hexokinase, although it has a complete pathway for glycolysis from glucose 6-phosphate or for gluconeogenesis. There are no enzymes for the classical or modified Entner-Doudoroff pathways that are found in many *Crenarchaeota*. The organism does have a modified ribulose monophosphate pathway to produce ribose 5-phosphate (23), and a standard pyrimidine biosynthetic pathway. However, it lacks genes for purine nucleotide biosynthesis. Finally, an extensive set of UDP-sugar biosynthesis proteins and glycosyltransferases suggests the presence of glycosylated proteins and lipids. Although “*Ca. K. cryptofilum*” appears to be a proficient peptide degrader, it has an extensive set of amino acid biosynthesis enzymes (see *SI Text*). However, there are many genes missing for coenzyme biosynthesis that are conserved in most of the other *Archaea*. For coenzyme A biosynthesis, it lacks the bifunctional phosphopantothoenylcysteine synthetase/decarboxylase that is found in all other sequenced archaeal genomes except for *Nanoarchaeum equitans* and *Thermofilum pendens* (24). In addition, pathways for riboflavin, pterin, lipoate, porphyrin, and quinone biosynthesis are incomplete.

**DNA Replication and Cell Cycle.** For initiating chromosome replication, two distinct *orc1/cdc6* homologues and a single minichromosome maintenance protein (MCM) complex are present along with genes encoding single-stranded binding protein (RPA) and primase (PriSL). The genome encodes multiple DNA-dependent, DNA polymerases including 2 family B type enzymes and both the large and small subunits of a euryarchaeal type II polymerase. Genes for the sliding clamp (PCNA), PriSL, and a *gins15* ortholog (25), are clustered with genes for the large subunit of the type II polymerase. A simplified clamp loader complex encodes the large and small subunits of replication factor C. Predicted chromatin-associated proteins include Alba and two H3-H4 histones. Like all known hyperthermophiles, reverse gyrase is present.

“*Ca. K. cryptofilum*” possesses several genes related to the ParA/MinD family of ATPases involved in chromosome partitioning and SMC-like proteins involved in chromosome segregation. The gene for this ATPase is part of a predicted operon that also includes genes for an FtsK-like ATPase (HerA) and two nucleases, proteins that are thought to comprise the basic machinery for DNA-pumping (26). The organism appears to employ the euryarchaeal mechanism for cell division as indicated by the presence of 7 genes encoding cell division GTPases (FtsZ; *SI Fig. 7*) (27). One of the *ftsZ* genes is included in a conserved euryarchaeal gene cluster containing *secE*, *nusG*, and several ribosomal protein genes (28, 29). In addition, 5 paralogous *ftsZ* genes are present in a 7-gene cluster that also includes a putative adapter protein (30).

**Transcription and Translation.** “*Ca. K. cryptofilum*” possesses a full complement of archaeal DNA dependent RNA polymerase (RNAP) subunits. The *rpoA* and *rpoB* genes encoding the

largest subunits of the RNAP are intact. In addition to the typical archaeal RNAP subunits, a coding region of 110 amino acids was identified with limited sequence similarity to the RPB8 of the eukaryotic RNAP. Subsequent in-depth analysis has shown that an ortholog of RPB8, previously thought to be missing in archaea, is also encoded by all sequenced genomes of hyperthermophilic *Crenarchaeota* (31). The RPB8 ortholog resides in a putative operon with the eukaryotic-like transcription factor, TFIIB. To initiate basal transcription, archaeal homologues for TATA-binding protein, transcription factor B (TFB), and transcription factor E (TFE) are present. Transcriptional regulators are of the bacterial/archaeal type, with the XRE, TrmB, ArsR, PadR-like, CopG, Lrp/AsnC, and MarA families represented in the genome.

The rRNA operon contains a SSU (16S) as well as a LSU (23S) which harbours an intron-encoded LAGLIDADG type homing endonuclease similar to crenarchaeal homologues (32). A total of 33 LSU ribosomal proteins (r-proteins) and 27 SSU r-proteins are present. Notably, r-proteins S30e, S25e, S26e, and L13e that are conserved in the *Crenarchaeota* but are absent in *Euryarchaeota* (33) were identified. In contrast, large subunit r-proteins L20a, L29, and L35ae are missing from the genome.

The tRNA set consists of one initiator tRNA and 45 non-redundant elongator tRNAs. An unusual tRNA<sup>Ile</sup> with an UAU anticodon is predicted to decode the ATA codon instead of a modified CAU commonly found in archaea (with the exception of *Nanoarchaeum equitans*) (34). Both selenocysteine and pyrrolysine-specific tRNAs are absent. Four tRNA genes contain an intron located one base downstream of the anticodon and one tRNA gene (tRNA<sup>Ser</sup> CGA) contains an intron in the D-loop. The structural splicing motifs found at all 5 exon-intron junctions and the corresponding homomeric splicing endonuclease appear to reflect the conserved splicing mechanism found in *Euryarchaeota* (35). Also similarly to some *Euryarchaeota*, the universal G-1 residue found at the 5' terminus of tRNA<sup>His</sup> is not encoded but is predicted to be added posttranscriptionally by a guanylyltransferase. The genome encodes archaeal aminoacyl-tRNA synthetases for all of the amino acids except for glutamyl-tRNA formation which is mediated via the tRNA-dependent transamidation pathway using the GatD and GatE proteins (36). The LysRS is of the class I type and a homodimeric GlyRS is present. The SerRS is the common type rather than the rarer version found in some methanogens (37). On the other hand, ThrRS appears to be a bacterial type and was likely acquired through a HGT event.

**Phylogeny and Evolutionary Genomics.** We performed a comprehensive phylogenetic analysis based on combined large and small rRNA subunits, conserved single-gene markers, and conserved concatenated proteins. Collectively, these results demonstrate that “*Ca. K. cryptofilum*” represents a deeply diverged archaeal lineage with affinity to the *Crenarchaeota*. Combined SSU+LSU rRNA subunit trees supported a deep crenarchaeal position (Fig. 2A). Likewise, the maximum likelihood based phylogeny of elongation factor 2 (EF2) homologues from archaeal genomes or environmental fosmid sequences corresponded with the rRNA tree (Fig. 2B). Phylogenetic analysis of 33 concatenated r-proteins and 3 large RNAP subunits clustered the korarchaeote with *C. symbiosum* in a deep branch joining the hyperthermophilic *Crenarchaeota* (Fig. 2C). However, this grouping could be a long branch attraction artifact, and a statistical test showed that a basal position of “*Ca. K. cryptofilum*” identical to that in Fig. 2A and 2B could not be ruled out. See SI Text for separate RNAP subunit and r-proteins phylogenies with compatibility testing.

## Discussion:

**Capturing a Korarchaeal Genome.** Critical improvements in the cultivation and *in-situ* identification were necessary to resolve a complete korarchaeal genome. The ultra-thin, filamentous organisms hybridizing to *Korarchaeota*-specific probes displayed a thinner and generally longer morphology than what has been previously described for pJP27-type korarchaeote (38). It is not known if the morphological discrepancies are due to differences in the enrichment conditions, hence growth rate, or if variation in cell shape occurs among closely related species. Nevertheless, SDS concentrations that are generally 5 to 50 fold higher than those that are typically required for FISH analyses of hyperthermophilic archaea (39) were necessary for optimal probe penetration. The structural integrity of “*Ca. K. cryptofilum*” in the presence of surfactants is likely attributed to the densely packed S-layer revealed through EM studies (Fig. 1D). Exploiting this feature allowed the filamentous cells to be sufficiently purified for WGS sequencing and assembly into a single contiguous chromosome. The proposed name for the organism reflects its elusive nature and reputation for hiding within its community and also for its ultra-thin, filamentous morphology. The proposed genus, *Korarchaeum* gen. nov., stems from the originally proposed phylum designation by Barns *et al.* (3), which is derived from the Greek noun, *koros* or *kore* meaning “young man” or “young woman” respectively; and the Greek adjective *archaios* for “ancient”. The proposed species name *cryptofilum* sp. nov., is derived from the Greek adjective, *kryptos*, meaning “hidden” and the Latin noun *filum*, “a thread”.

**Metabolism.** Determining the growth requirements in detail for “*Ca. K. cryptofilum*” was not possible since the organism could only be propagated in a complex enrichment culture. Isolation attempts using Gelrite plates, dilution series, or optical tweezers were unsuccessful. However, the major aspects of the metabolism could be reconstructed from the predicted set of protein-coding genes which suggest an obligately anaerobic, heterotrophic lifestyle with peptides serving as the principal carbon and energy source. In agreement with the predicted metabolism, the enrichment culture was supplied with peptone and traces of yeast extract as the primary carbon and energy source under strictly anaerobic conditions. Anaerobic peptide utilization is a common metabolic strategy among hyperthermophilic *Crenarchaeota* and *Euryarchaeota* (40) and has been characterized in detail in the model organism *Pyrococcus furiosus* (41-44). However, “*Ca. K. cryptofilum*” apparently differs from other known hyperthermophiles in lacking the ability to utilize exogenous electron acceptors such as oxygen, nitrate, iron, or sulfur (45). Protons appear to be the primary acceptor for ferredoxin-shuttled electrons. To avert possible growth inhibition, removal of molecular hydrogen by flushing with N<sub>2</sub>/CO<sub>2</sub> gas and also by possible hydrogen consuming members of the enrichment community such as *Archaeoglobus* and *Thermodesulfobacterium* spp. might have improved cell growth. The organism also appears to lack complete pathways for the *de novo* synthesis of several cofactors which may prevent growth in axenic cultures. These coenzymes must be scavenged from the environment or the organism has evolved alternative modes for producing them. Microbial communities forming high-density mats composed of filamentous cells have yielded the highest number of amplified korarchaeal SSU rDNAs (9-11). Some of the essential nutrients for the growth might be supplied *in-situ* by other mat-forming organisms.



**Evolutionary Considerations.** Independent phylogenetic analyses based on combined SSU+LSU rRNA, elongation factor 2 (EF-G/EF-2), and concatenated r-proteins + RNAP subunit sequences are compatible with the notion of the *Korarchaeota* being a deeply branching lineage with affinity to the *Crenarchaeota* (Fig. 2). This genome-based assessment corroborates a previous phylogenetic analysis based on a robust set of archaeal environmental SSU rDNA sequences (46). The apparent relationship between the *Korarchaeota* and a member of the marine group 1 *Crenarchaeota* suggested by the phylogeny of concatenated r-protein + RNAP subunits (Fig. 2C) is of potential interest. Based on comprehensive phylogenetic analyses and gene content comparisons, the mesophilic *Crenarchaeota* have recently been proposed to form a separate major phylum within the Archaea (47). The apparent affinity between *C. symbiosum* and “*Ca. K. cryptofilum*” presented in our analysis remains to be validated since whole-genome phylogenetic reconstructions are based on a limited number of available archaeal genomes.

The genome revealed a pattern of orthologs that suggests an early divergence within the archaeal domain. The complement of information processing and cell cycle components appears to be a hybrid, with proteins composing the ribosome and RNAP shared, primarily, with *Crenarchaeota*, whereas functions involving tRNA maturation, DNA replication/repair, and cell division being more typical of the *Euryarchaeota* (Table 2). This complex pattern could have resulted from a combination of vertically inherited traits from ancestral organisms supplemented by HGT events. Recent genome analyses have shown that genes believed to be exclusive to the *Euryarchaeota* are also present in some crenarchaeotes. For example, a type-II DNA polymerase and a divergent *ftsZ* homologue are present in *Cenarchaeum symbiosum* (48), and histones are also found in mesophilic and some hyperthermophilic *Crenarchaeota* (49, 50). It remains to be determined whether these genes were vertically inherited from a common archaeal ancestor or were acquired horizontally from members of the *Euryarchaeota* or Bacteria (51). The euryarchaeal type features found in “*Ca. K. cryptofilum*” are generally more similar to those found in thermophilic and hyperthermophilic *Euryarchaeota* (SI Table 6). The presence of several mobile elements in the genome certainly suggests that the gene content may have been influenced by HGT (SI Text). Sequencing additional archaeal genomes will aid in determining whether the amalgam of cren- and euryarchaeal characteristics present in the korarchaeal genome represents an ancient feature or resulted from a combination of HGT and gene loss events. More than a decade after the *Korarchaeota* were introduced based on rDNA sequences (2, 3), identifying “*Ca. K. cryptofilum*” and sequencing its genome has provided a new perspective into the biological diversity of these elusive organisms and the genomic complexity of the archaeal domain.

## Materials and Methods:

**Sample Collection and Cultivation.** Sediment and water samples were collected by B.P.H. from Obsidian Pool, Yellowstone National Park, USA, and ranged from 78°-92° C with a pH of ca. 6.5. The cultivation conditions for the Obsidian Pool enrichment culture were similar to those described previously (38). For details see SI Text.

**Fluorescence *In-situ* Hybridization Analysis.** FISH analysis was performed similar to described previously (39). Cy3-labeled, oligonucleotide probes KR515R (CCAGCCTTACCCCTCCCCT) and KR565R (AGTATGCGTGGGAACCCCTC) provided optimal results. The hybridization solution containing 0.9 M NaCl, 0.5% SDS, 100 µg/ml

sheared herring sperm DNA, 0.02 M Tris-HCl (pH 7.2), and 20% formamide (v/v). The wash buffer containing 0.23 M NaCl, 0.1% (w/v) SDS, and 0.02 M Tris-HCl (pH 7.2). For details see *SI Text*.

**Electron Microscopy.** Cell pellets were immediately fixed in a solution containing 2.5% glutaraldehyde (EM grade) in 20 mM sodium cacodylate buffer (pH 6.5). EM method details are provided in *SI Text*.

**Cell Purification.** Fermentor effluent was collected in sterile 2 l glass bottles. Washed cells were briefly exposed to 0.2% SDS (w/v) and then washed 3 times with PBS (pH 7.2). Cell suspensions were then filtered through 0.45  $\mu$ m syringe filters (MILLEX HV, Millipore, Ireland) in 25 ml aliquots. The filtrate was centrifuged at 6000 rpm for 30 min. to collect the cells. See *SI Text* for detailed protocol.

**Genome Sequencing and Assembly.** Library construction, sequencing, and assembly were performed at the Joint Genome Institute, Walnut Creek, CA, USA. See *SI Text*.

**Comparative Genomics and Phylogenetic Analyses.** The predicted protein-coding genes were compared against those from other genomes available in the Integrated Microbial Genomes (IMG) analysis tool (52) and the National Center for Biotechnology Information database. Archaeal COGs were analyzed using the COGNITOR methods (19, 20, 53). An alignment of concatenated small and large subunit rRNA sequences (SSU+LSU rRNA) was constructed based on their conserved secondary structures and refined by hand. See *SI Text* for detailed information regarding phylogenetic analysis and tree construction.

This paper is dedicated to Carl Woese on the occasion of his 80<sup>th</sup> birthday. We thank Norman Pace for insightful comments regarding preparation of the final manuscript. We also thank the JGI production sequencing team; plus, Miriam Land and the Computational Biology Group at ORNL. Funding was provided to J.G.E and K.O.S. by Verenum (formerly Diversa) Corporation, San Diego, California, and The Deutsche Forschungsgemeinschaft. Support for genome sequencing and assembly was provided by the U.S. Dept. of Energy and the JGI Community Sequencing Program. Support to B.P.H. was provided by the Alexander von Humboldt Foundation and NSF no. MCB-0546865.

## References:

1. Woese CR, Kandler O, Wheelis ML (1990) Towards a natural system of organisms: proposal for the domains Archaea, Bacteria, and Eucarya. *Proc Natl Acad Sci USA* 87:4576-4579.
2. Barns SM, Fundyga RE, Jeffries MW, Pace NR (1994) Remarkable archaeal diversity detected in a Yellowstone National Park hot spring environment. *Proc Natl Acad Sci USA* 91:1609-1613.
3. Barns SM, Delwiche CF, Palmer JD, Pace NR (1996) Perspectives on archaeal diversity, thermophily and monophyly from environmental rRNA sequences. *Proc Natl Acad Sci USA* 93:9188-9193.

4. Auchtung TA, Takacs-Vesbach CD, Cavanaugh CM (2006) 16S rRNA phylogenetic investigation of the candidate division "Korarchaeota". *Appl Environ Microbiol* 72:5077-5082.
5. Takai K, Horikoshi K (1999) Genetic diversity of archaea in deep-sea hydrothermal vent environments. *Genetics* 152:1285-1297.
6. Inagaki F, *et al.* (2003) Microbial communities associated with geological horizons in coastal subseafloor sediments from the sea of Okhotsk. *Appl Environ Microbiol* 69:7224-7235.
7. Waters E, *et al.* (2003) The genome of *Nanoarchaeum equitans*: insights into early archaeal evolution and derived parasitism. *Proc Natl Acad Sci USA* 100:12984-12988.
8. Brochier C, Gribaldo S, Zivanovic Y, Confalonieri F, Forterre P (2005) Nanoarchaea: representatives of a novel archaeal phylum or a fast-evolving euryarchaeal lineage related to Thermococcales? *Genome Biol* 6:R42.
9. Reysenbach AL, Ehringer M, Hershberger K (2000) Microbial diversity at 83 degrees C in Calcite Springs, Yellowstone National Park: another environment where the Aquificales and "Korarchaeota" coexist. *Extremophiles* 4:61-67.
10. Hjorleifsdottir S, Skirnisdottir S, Hreggvidsson GO, Holst O, Kristjansson JK (2001) Species composition of cultivated and noncultivated bacteria from short filaments in an Icelandic hot spring at 88 degrees C. *Microb Ecol* 42:117-125.
11. Skirnisdottir S, *et al.* (2000) Influence of sulfide and temperature on species composition and community structure of hot spring microbial mats. *Appl Environ Microbiol* 66:2835-2841.
12. Takai K, Yoshihiko S (1999) A molecular view of archaeal diversity in marine and terrestrial hot water environments. *FEMS Microbiol Ecol* 28:177-188.
13. Marteinsson VT, *et al.* (2001) Discovery and description of giant submarine smectite cones on the seafloor in Eyjafjordur, northern Iceland, and a novel thermal microbial habitat. *Appl Environ Microbiol* 67:827-833.
14. Schrenk MO, Kelley DS, Delaney JR, Baross JA (2003) Incidence and diversity of microorganisms within the walls of an active deep-sea sulfide chimney. *Appl Environ Microbiol* 69:3580-3592.
15. Nercessian O, Reysenbach AL, Prieur D, Jeanthon C (2003) Archaeal diversity associated with in situ samplers deployed on hydrothermal vents on the East Pacific Rise (13 degrees N). *Environ Microbiol* 5:492-502.
16. Spear JR, Walker JJ, McCollom TM, Pace NR (2005) Hydrogen and bioenergetics in the Yellowstone geothermal ecosystem. *Proc Natl Acad Sci USA* 102:2555-2560.
17. Teske A, *et al.* (2002) Microbial diversity of hydrothermal sediments in the Guaymas Basin: evidence for anaerobic methanotrophic communities. *Appl Environ Microbiol* 68:1994-2007.
18. Lowe TM, Eddy SR (1997) tRNAscan-SE: a program for improved detection of transfer RNA genes in genomic sequence. *Nucleic Acids Res* 25:955-964.
19. Makarova KS, Sorokin AV, Novichkov PS, Wolf YI, Koonin EV (2007) Clusters of orthologous genes for 41 archaeal genomes and implications for evolutionary genomics of archaea. *Biol Direct* 2:33.
20. Tatusov RL, *et al.* (2003) The COG database: an updated version includes eukaryotes. *BMC Bioinformatics* 4:41-54.
21. Saprà R, Bagramyan K, Adams MWW (2003) A simple energy-conserving system: Proton reduction coupled to proton translocation. *Proc Natl Acad Sci USA* 100:7545-7550.
22. Lindahl PA, Graham DE (2007) in *Nickel and Its Surprising Impact in Nature*, eds Sigel A, Sigel H, Sigel RKO (John Wiley & Sons, Chichester, UK), pp. 357-416.

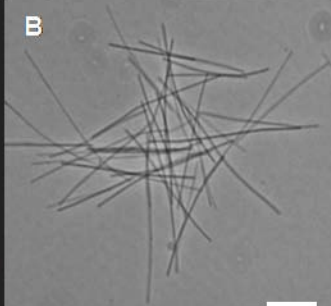
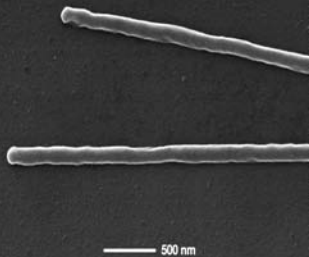
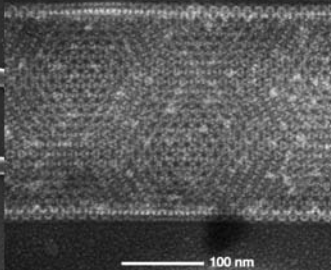
23. Orita I, *et al.*, (2006) The Ribulose Monophosphate Pathway Substitutes for the Missing Pentose Phosphate Pathway in the Archaeon *Thermococcus kodakaraensis*. *J. Bacteriol.* 188:4698-4704.
24. Anderson I, *et al.* (2008) Genome sequence of *Thermofilum pendens* reveals an exceptional loss of biosynthetic pathways without genome reduction. *J Bacteriol.* E-pub
25. Marinsek N, *et al.* (2006) GINS, a central nexus in the archaeal DNA replication fork. *EMBO Rep* 7:539-545.
26. Iyer LM, Makarova KS, Koonin EV, Aravind L (2004) Comparative genomics of the FtsK-HerA superfamily of pumping ATPases: implications for the origins of chromosome segregation, cell division and viral capsid packaging. *Nucleic Acids Res* 32:5260-5279.
27. Vaughan S, Wickstead B, Gull K, Addinall SG (2004) Molecular evolution of FtsZ protein sequences encoded within the genomes of archaea, bacteria, and eukaryota. *J Mol Evol* 58:19-29.
28. Faguy DM, Doolittle WF (1998) Cytoskeletal proteins: the evolution of cell division. *Curr Biol* 8:R338-341.
29. Poplawski A, Gullbrand B, Bernander R (2000) The *ftsZ* gene of *Haloferax mediterranei*: sequence, conserved gene order, and visualization of the FtsZ ring. *Gene* 242:357-367.
30. Ye H, *et al.* (2004) Crystal structure of the putative adapter protein MTH1859. *J Struct Biol* 148:251-256.
31. Koonin EV, Makarova KS, Elkins JG (2007) Orthologs of the small RPB8 subunit of the eukaryotic RNA polymerases are conserved in hyperthermophilic Crenarchaeota and "Korarchaeota". *Biology Direct* 2.
32. Cann IK, Ishino S, Nomura N, Sako Y, Ishino Y (1999) Two family B DNA polymerases from *Aeropyrum pernix*, an aerobic hyperthermophilic crenarchaeote. *J Bacteriol* 181:5984-5992.
33. Lecompte O, Ripp R, Thierry JC, Moras D, Poch O (2002) Comparative analysis of ribosomal proteins in complete genomes: an example of reductive evolution at the domain scale. *Nucleic Acids Res* 30:5382-5390.
34. Marck C, Grosjean H (2002) tRNomics: analysis of tRNA genes from 50 genomes of Eukarya, Archaea, and Bacteria reveals anticodon-sparing strategies and domain-specific features. *RNA* 8:1189-1232.
35. Parrish J, *et al.* (2001) Mitochondrial endonuclease G is important for apoptosis in *C. elegans*. *Nature* 412:90-94.
36. Feng L, Sheppard K, Tumbula-Hansen D, Söll D (2005) Gln-tRNAGln Formation from Glu-tRNAGln Requires Cooperation of an Asparaginase and a Glu-tRNAGln Kinase. *J Biol Chem* 280:8150-8155.
37. Kim HS, Vothknecht UC, Hedderich R, Celic I, Söll D (1998) Sequence divergence of seryl-tRNA synthetases in archaea. *J Bacteriol* 180:6446-6449.
38. Burggraf S, Heyder P, Eis N (1997) A pivotal Archaea group. *Nature* 385:780.
39. Burggraf S, *et al.* (1994) Identifying members of the domain Archaea with rRNA-targeted oligonucleotide probes. *Appl Environ Microbiol* 60:3112-3119.
40. Kelly RM, Adams MW (1994) Metabolism in hyperthermophilic microorganisms. *Antonie Van Leeuwenhoek* 66:247-270.
41. Ma K, Schicho RN, Kelly RM, Adams MW (1993) Hydrogenase of the hyperthermophile *Pyrococcus furiosus* is an elemental sulfur reductase or sulfhydrogenase: evidence for a sulfur-reducing hydrogenase ancestor. *Proc Natl Acad Sci USA* 90:5341-5344.

42. Mai X, Adams MW (1994) Indolepyruvate ferredoxin oxidoreductase from the hyperthermophilic archaeon *Pyrococcus furiosus*. A new enzyme involved in peptide fermentation. *J Biol Chem* 269:16726-16732.
43. Blamey JM, Adams MW (1993) Purification and characterization of pyruvate ferredoxin oxidoreductase from the hyperthermophilic archaeon *Pyrococcus furiosus*. *Biochim Biophys Acta* 1161:19-27.
44. Schut GJ, Brehm SD, Datta S, Adams MW (2003) Whole-genome DNA microarray analysis of a hyperthermophile and an archaeon: *Pyrococcus furiosus* grown on carbohydrates or peptides. *J Bacteriol* 185:3935-3947.
45. Huber R, Huber H, Stetter KO (2000) Towards the ecology of hyperthermophiles: biotopes, new isolation strategies and novel metabolic properties. *FEMS Microbiol Rev* 24:615-623.
46. Robertson CE, Harris JK, Spear JR, Pace NR (2005) Phylogenetic diversity and ecology of environmental Archaea. *Curr Opin Microbiol* 8:638-642.
47. Brochier-Armanet C, Boussau B, Gribaldo S, Forterre P (2008) Mesophilic crenarchaeota: proposal for a third archaeal phylum, the Thaumarchaeota. *Nat Rev Microbiol* 6:245-252.
48. Hallam SJ, *et al.* (2006) Genomic analysis of the uncultivated marine crenarchaeote *Cenarchaeum symbiosum*. *Proc Natl Acad Sci USA* 103:18296-18301.
49. Cubonova L, Sandman K, Hallam SJ, Delong EF, Reeve JN (2005) Histones in crenarchaea. *J Bacteriol* 187:5482-5485.
50. Sandman K, Reeve JN (2006) Archaeal histones and the origin of the histone fold. *Curr Opin Microbiol* 9:520-525.
51. Lopez-Garcia P, Brochier C, Moreira D, Rodriguez-Valera F (2004) Comparative analysis of a genome fragment of an uncultivated mesopelagic crenarchaeote reveals multiple horizontal gene transfers. *Environ Microbiol* 6:19-34.
52. Markowitz VM, *et al.* (2006) The integrated microbial genomes (IMG) system. *Nucleic Acids Res* 34:D344-348.
53. Tatusov RL, Koonin EV, Lipman DJ (1997) A genomic perspective on protein families. *Science* 278:631-637.

**Figure legends:**

**Fig. 1.** Microscopy of “*Ca. K. cryptofilum*”. (A) FISH analysis with *Korarchaeota*-specific Cy3-labeled oligonucleotide probes KR515R/KR565R. The undulated cell shape results from drying of the specimen on gelatin coated slides prior to hybridization. Scale bar represents 5  $\mu\text{m}$ . (B) Phase contrast image of korarchaeal filaments following physical enrichment. Scale bar represents 5  $\mu\text{m}$ . (C), Scanning electron micrograph of purified cells. (D) Transmission electron micrograph after negative staining with uranyl acetate displaying the paracrystalline S-layer. Cells are flattened which increases their apparent thickness.

**Fig. 2.** Phylogenetic analysis of “*Ca. K. cryptofilum*”. (A) Maximum likelihood phylogenetic tree of combined (SSU+LSU) rRNAs rooted with corresponding bacterial sequences. Numbers at the nodes indicate bootstrap support. (B) Archaeal phylogeny based on translation elongation factor 2 (EF2) proteins rooted with bacterial homologs. The numbers indicate bootstrap support for PhyML/consensus posterior probability (Phyloblast), an asterisk indicates <50 bootstrap support. Where both values were <50, the branch was collapsed. (C) Maximum likelihood tree made from aligned sequences of 33 universally conserved ribosomal proteins and the 3 largest RNA polymerase subunits, RpoA, RpoB, and RpoD. Bootstrap support numbers are given at the nodes as a percentage ( $n=10000$ ). Scale bars represent the average number of substitutions per residue.

**A****B****C****D**

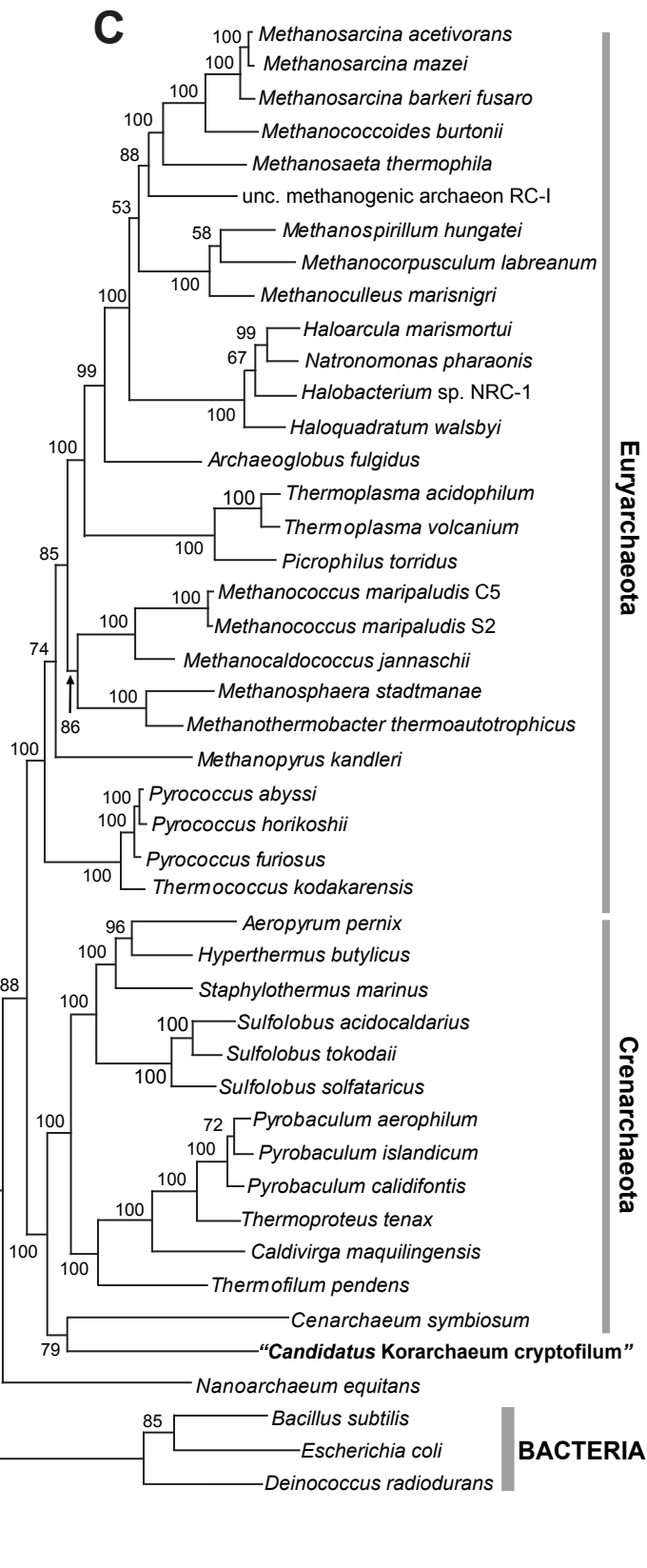
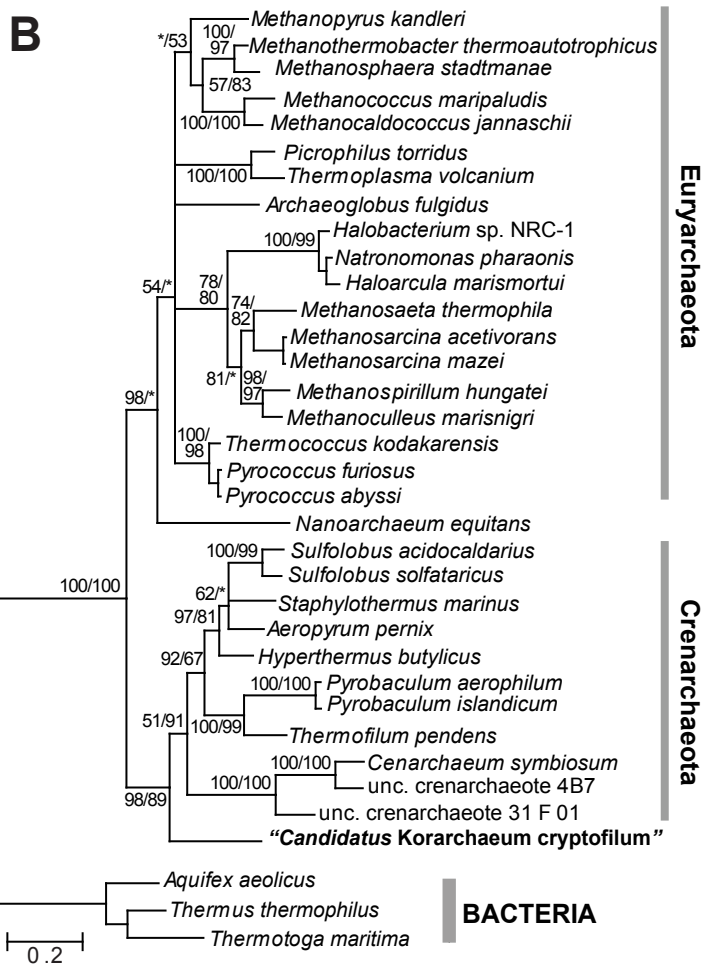
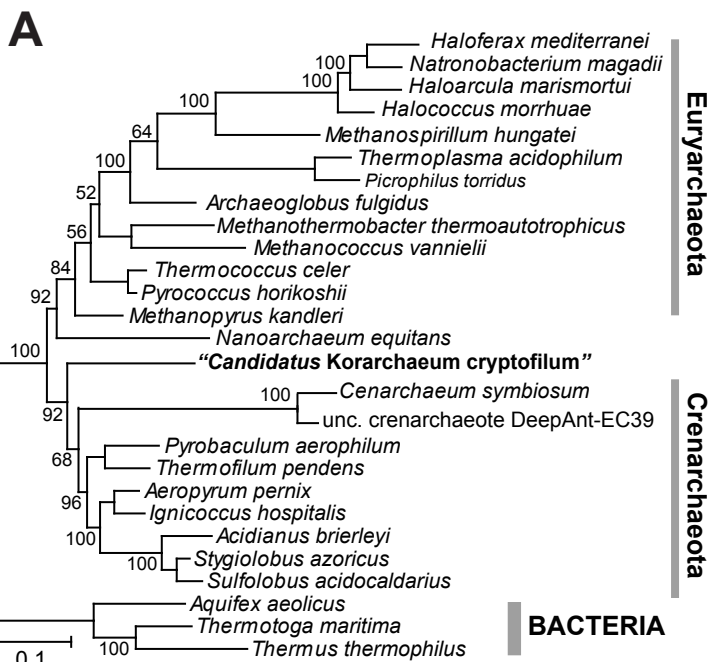




**Table 1. General features of the “*Ca. K. cryptofilum*” genome**

Total number of bases	1590757
Coding density (%)	89
G + C content (%)	49
Total number of predicted genes	1661
Protein coding genes	1602
Average ORF length (bp)	870
rRNA genes*	3
tRNA genes	45
Genes assigned to COGs	1401
Genes assigned to arCOGs	1382
Genes with function prediction	998
Genes with biochemical prediction only	246
Genes with unknown function or activity	358

---

\*16S, 23S, and 5S rRNA

**Table 2. Crenarchaeal and euryarchaeal arCOGs in “*Ca. K. cryptofilum*”**

arCOG	Cat.*	Function	Eu <sup>‡</sup>	Cr <sup>§</sup>
04447	L	DNA polymerase II, large subunit	27	0
04455	L	DNA polymerase II, small subunit	26	0
00872	L	ERCC4-like helicase	26	0
02610	L	Rec8/ScpA/Sccl-like protein	24	0
02258	L	subunit of RPA complex	20	0
00371	D	Chromosome segregation ATPase, SMC	24	0
02201	D	Cell division GTPase FtsZ	26	0
01013	J	Protein with L13E-like domain	0	11
04327	J	Ribosomal protein S25	0	13
04293	J	Ribosomal protein S30	0	13
04305	J	Ribosomal protein S26	0	13
04271	K	RNA polymerase, subunit RPB8	0	12
00393	K	Membrane-associated transcriptional regulator	0	9

\*COG functional categories: L, Replication, recombination and repair; D, Cell cycle control, cell division, chromosome partitioning; J, Translation, ribosomal structure and biogenesis; K, Transcription. <sup>‡</sup>Number of euryarchaeal (Eu) genomes containing that arCOG (out of 27 total). <sup>§</sup>Number of crenarchaeal (Cr) genomes containing that arCOG (13 total).

## Supporting Text

### Results:

**Cultivation and Cell Identification.** Members of the Crenarchaeota were represented by clone types pOPF\_10, pOPF\_07, and pOPF\_12 (OPF = Obsidian Pool Fermentor) which shared 98% similarity to *Thermosphaera aggregans* strain M11TL<sup>T</sup> (1); 98% similarity to *Thermofilum pendens* S10TFL (1); and 98% similarity to an uncultured *Pyrobaculum* sp. HVerd019N respectively (Kvist, 2006; unpublished). Two closely related organisms within the Euryarchaeota were designated pOPF\_1 and pOPF\_3 and were 98% and 99% similar, respectively, to an uncultivated member of the Archaeoglobales from Obsidian Pool designated OPPDO15 (2). A single member of the *Korarchaeota*, represented by the 16S rDNA clone pOPF\_08, was supported by the enrichment culture. The 16S sequence of this “korarchaeote” is 99% similar to both the pJP27 sequence type from Obsidian Pool, YNP (3), and the pAB5 sequence from Calcite Springs, YNP (4) (see SI Fig. 3).

**FISH Analysis.** Cy3-labeled, oligonucleotide probes (5’-3’) KR515R (CCAGCCTTACCCTCCCCT) and KR565R (AGTATGCGTGGGAACCCCTC) allowed visualization of the korarchaeal filamentous cells in single probe hybridizations but provided the best results when applied in combination. A crenarchaeota-specific probe, CREN499R (CCARNCTTGCCCCCGCT) labelled with Alexa488, failed to hybridize to KR515R/KR565R positive filaments however showed bright fluorescence when pure cultures of *Thermofilum* sp. S10TFL were used as a positive control (SI Figs. 4A and 4B). Probes KR515R and KR565R did not hybridize to pure cultures of *Thermofilum* sp. S10TFL. Domain specific probes ARC915 (5’-GTGCTCCCCCGCCAATTCCT-3’) (5) and EUB338 (5’-GCTGCCTCCCGTAGGAGT-3’) (6) also did not hybridize to the *Korarchaeota* positive filaments (data not shown). Addition of sheared fish sperm DNA to the hybridization buffer reduced background fluorescence. The SDS concentration in the hybridization buffer had to be increased to 0.5% (w/v) to allow sufficient probe penetration.

**Sequencing and Assembly.** Sample sequencing was used to determine which libraries represented the highest number of korarchaeal genomic sequences. The fraction of end-reads that aligned with the 84.7 kb korarchaeal genomic contig (SI Fig. 6) was determined. Libraries BFPP and especially BHXI yielded the highest proportion of sequences that overlapped with the korarchaeal 84.7 kb contig and were selected for further sequencing. A total of 23,000 and 11,520 sequencing reads were produced from the BHXI and BFPP libraries respectively. The average read length was 800 +/- 113 bp for the small-insert BHXI library and 625 +/- 170 bp for the fosmid based BFPP library. A high number of reads (2292) from the BFPP library were of insufficient length and were not used for further analysis. An additional 6184 sequencing reads from the BFPP library were also determined to be from other Obsidian Pool enrichment culture organisms (based on %GC analysis) and were therefore rejected. Attempts at assembling the “*Candidatus* Korarchaeum cryptofilum” genome were made using the 23000 quality sequencing reads from the BHXI library combined with 3044 reads from the large-insert library. From the assembly data, it was evident that the original DNA sample contained a dominant genome represented by the pOPF\_08 clone type and at least two other genomic variants in low concentration. Since the dominate genome was sufficiently

enriched relative to other variants (approximately 10-fold), genomic heterogeneity did not prevent the assembly of the complete genome of the pOPF\_08 organism.

**Amino Acid Biosynthesis.** Although “*Ca. K. cryptofilum*” appears to be a proficient peptide degrader, it has an extensive set of amino acid biosynthesis enzymes. The predicted repertoire includes a canonical branched chain amino acid pathway and redundant threonine dehydratase and citramalate synthases to produce 2-oxobutyrate, the precursor for isoleucine biosynthesis. Similar to crenarchaeotes and the *Thermococcales*, “*Ca. K. cryptofilum*” appears to use the homocitrate pathway and genes of the *lysYZWXJK* operon to produce lysine (7). However, it also encodes *dapA*, *dapE*, *dapC*, and *lysA* homologs from the diaminopimelate pathway of lysine synthesis although *dapB*, *dapD*, and *dapF* genes are missing. Also missing are histidine and tryptophan biosynthesis genes, although the prephenate pathway to phenylalanine and tyrosine is complete. Unlike the known Crenarchaeota, the korarchaeote is predicted to use the methanogenic version of chorismate synthesis (8). Common pathways are available to produce arginine, proline, threonine, and serine can be made through the phosphorylating pathway.

**Mobile Elements.** The “*Ca. K. cryptofilum*” genome contains 6 genes (Kcr\_0344, Kcr\_0272, Kcr\_1558, Kcr\_0611, Kcr\_1387, Kcr\_0856) that encode OrfB of the IS605 family of transposases (9) which are widespread throughout the Archaea (10). Kcr\_1558 and Kcr\_1387 share 87% identity and both alleles are clustered with predicted ISC1913-like elements similar to those found in *Sulfolobus solfataricus* P2 (11). Kcr\_0344 and Kcr\_0272 are also nearly identical to one another and are closely related to IS605 sequences found in hyperthermophilic crenarchaeotes as well as transposable elements carried by conjugal plasmids (12).

**Tree Compatibility.** Analysis of concatenated protein alignments hinges on the assumption that the true phylogenies of all genes involved are the same and the observed differences between trees reconstructed from individual genes represent noise. Thus, ideally, genes must be tested for compatibility of their individual phylogenies before concatenation. Practically, when dealing with large set of genes, such as >30 r-proteins and 6 RNAP subunits, complete rigorous testing becomes unfeasible. Thus we employed the following scheme:

The 6 RNAP subunit alignments were concatenated, and an ML phylogenetic tree was reconstructed from the concatenated alignment. Each original alignment was tested for compatibility with the topology of this tree using the Approximately Unbiased (AU) test (13) as implemented in the TreeFinder program (14). Three subunits (E', F and N) were found to be incompatible with the concatenated tree and, accordingly, were rejected; three ( $\beta$  and two chains of  $\beta'$ ) passed the test (data not shown). The concatenated alignment of these three subunits was used in all further analyses.

Individual ribosomal proteins are generally too short to be used for a meaningful phylogenetic reconstruction individually, so their alignments were concatenated without detailed testing. We further assessed the compatibility of phylogenetic tree topologies between the concatenated r-proteins and concatenated RNAP subunits. First, *M. kandleri* sequences were removed from both datasets as it has been shown earlier that translational and transcriptional machineries of this archaeon appear to be of different origins (15). Maximum likelihood phylogenetic trees were

reconstructed for the concatenated r-proteins, concatenated RNAP subunits, and the two protein sets concatenated together. All three reconstructions placed “*Ca. K. cryptofilum*”, *C. symbiosum* and *N. equitans* into slightly different deep positions in the archaeal tree. Each of the three reconstructed phylogenies was reduced to an "essential constraint" tree which preserves the deep branching order of “*Ca. K. cryptofilum*”, *C. symbiosum*, *N. equitans*, Crenarchaeota clade, the Euryarchaeota clade, and the Bacteria clade but reduces the rest of the tree to a polytomies. Multifurcations in each of the three constraint trees were resolved separately for the concatenated r-proteins and concatenated RNAP subunits. Each of the two protein sets was tested for compatibility with two alternative topologies against its native topology using the AU test.

The tree topologies of concatenated r-proteins and concatenated RNAP subunits were mutually incompatible (AU p-value is <0.0001 for both cross comparisons). However, each topology was compatible with the topology of the joint tree that was obtained from the concatenation of both alignments (AU p-value of 0.44 for the r-proteins and 0.09 for the RNAP subunits). This concatenation provides the "middle ground" topology which is compatible with both original components.

For compatibility testing, the trees are given below in the Newick format or can be represented as rooted or unrooted trees using the TreeView program (<http://taxonomy.zoology.gla.ac.uk/rod/treeview.html>)

Rib+Rpo:

```
((((((((Aerpe:0.36773495,Hypbu:0.21297609):0.058441252,Stama:0.27448517):0.066622257,((Sulac:0.15015128,Sulto:0.10456212):0.069624523,Sulso:0.1509329):0.2630078):0.08883196,((Calm a:0.3253224,((Pyrae:0.054856231,Pyris:0.067626872):0.025078936,Pyrc a:0.059170292):0.10683526,The te:0.15772165):0.15116257):0.19498017,Thepe:0.3837574):0.091744444):0.084763622,(Censy:0.76822737,Korar:0.6614682):0.069591385):0.072259578,(((Bacsu:0.33698426,Escco:0.44608078):0.10326424,Deira:0.41947042):1.5273464,Naneq:0.64862503):0.086190568):0.066019763,(((Pyrab:0.012910551,Pyrho:0.022003269):0.01624607,Pyrfu:0.023925165):0.052710879,Theko:0.081936192):0.25734593):0.055934894,((Arcfu:0.34082045,((((Halma:0.11561483,Natph:0.1182512):0.038811422,Halsp:0.13959571):0.038397559,Halwa:0.14293013):0.40280754,Uncme:0.28868764):0.040151522,(((Metac:0.019253391,Metma:0.02656954):0.019116731,Metba:0.040855086):0.1295261,Metbu:0.18549369):0.1495346,Metsa:0.2967868):0.049075929):0.039992591),(Metcu:0.16004155,(Methu:0.19810155,Metla:0.26673314):0.036847236):0.24328027):0.097104881):0.070349984,(Picto:0.21986978,(Theac:0.070725281,Thevo:0.069452574):0.15861092):0.44427765):0.060677377,((Metja:0.14230929,(MetmC:0.015643543,Metmp:0.014565799):0.25379213):0.19458358,(Metst:0.23903843,Metth:0.1303759):0.23852987):0.041906053);
```

Rib:

```
((((((((Aerpe:0.31980804,Hypbu:0.20615681):0.055498529,Stama:0.25718752):0.066253714,((Sulac:0.16576925,Sulto:0.11668129):0.077594061,Sulso:0.16282142):0.28501161):0.093247323,((C
```

alma:0.33193714,(((Pyrae:0.057120572,Pyris:0.07077073):0.026296476,Pyrc:0.066530324):0.10905667,The:0.17545736):0.1438332):0.18642503,Thepe:0.38173286):0.099866176):0.085274407,(Censy:0.82794032,Korar:0.56696967):0.068304266):0.07088327,Naneq:0.68565168):0.044133173,((Bacsu:0.33527378,Escco:0.45321524):0.098950092,Deira:0.41249964):1.3966304):0.033603488,(((Arcfu:0.37551694,(((Halma:0.13342765,Natph:0.1326585):0.043048517,Halsp:0.15745755):0.043228326,Halwa:0.15991492):0.42703979,(Metcu:0.18289195,(Methu:0.22837977,Meta:0.29610791):0.043372113):0.21833222):0.035515818,(((Metac:0.021885312,Metma:0.027189481):0.020552123,Metba:0.047812763):0.13917693,Metbu:0.19809341):0.16309816,Metsa:0.34037388):0.049836532,Uncme:0.34735559):0.03902647):0.10982473):0.060987418,(Picto:0.23763709,(Theac:0.084552977,Thevo:0.085595389):0.18410383):0.45236938):0.058668401,((Metja:0.14052579,(MetmC:0.015882315,Metmp:0.015780284):0.26479904):0.18936641,(Metst:0.25169702,Metth:0.13607037):0.22555101):0.039398826):0.057778373,(((Pyrab:0.014396699,Pyrho:0.024345608):0.014770393,Pyrfu:0.020655354):0.056742521,Theko:0.0853559):0.24336287);

Rpo:

(((((((Aerpe:0.52456895,Hypbu:0.24236839):0.069374313,Stama:0.33298331):0.068457671,((Sulac:0.11654009,Sulto:0.077091543):0.052514386,Sulso:0.12574242):0.21556208):0.07859586,((Calm:0.31876506,(((Pyrae:0.050389173,Pyris:0.062111294):0.022680793,Pyrc:0.042864628):0.10570598,The:0.11873635):0.17435016):0.2250776,Thepe:0.40257348):0.072575108):0.077953824,Censy:0.71857094):0.064825184,(((Bacsu:0.34625103,Escco:0.4453692):0.10840656,Deira:0.46139837):2.2483465,(Korar:0.90258868,Naneq:0.75175588):0.10023721):0.060014185):0.072094977,(((Pyrab:0.0096322551,Pyrho:0.016736461):0.019982278,Pyrfu:0.033581242):0.043467586,Theko:0.076615985):0.3032898):0.054780751,((Arcfu:0.27501647,(((Halma:0.076647508,(Halsp:0.099864933,Halwa:0.12959176):0.030925598):0.02240101,Natph:0.067741209):0.36352804,(((Metac:0.013346087,Metma:0.025591969):0.015592053,Metba:0.024615296):0.10901293,Metbu:0.16095282):0.12200913,Metsa:0.20025675):0.038264588,(((Metcu:0.12050679,Methu:0.13685102):0.032523153,Meta:0.18647727):0.26028804,Uncme:0.21766027):0.038322895):0.047884765):0.073732157):0.094247225,(Picto:0.18714592,(Theac:0.039550499,Thevo:0.033687756):0.10319597):0.43834352):0.063219904,((Metja:0.15386209,(MetmC:0.016300163,Metmp:0.010996696):0.23172211):0.21688718,(Metst:0.21362919,Metth:0.12149914):0.28171906):0.050458485);

## Supporting Materials and Methods:

**Sample Collection and Cultivation.** A variety of sediment and water samples were collected from Obsidian Pool, Yellowstone National Park, Wyoming, USA, and ranged from 78°-92° C and had a pH of ca. 6.5. Similar samples collected near the same time our samples were taken (within days) were subjected to a detailed geochemical analysis by Schock et al. (16). The enrichment culture was established by adding several reduced and nonreduced samples (approximately 400 ml) of sediment and spring water to a double-walled glass vessel with a total volume of ca. 800 ml. The inoculation was performed inside a Coy anaerobic tent (Coy Laboratories, Grass Lake, MI, USA) to avoid exposure to air. Heated glycerol was pumped through the outer chamber of the

vessel to maintain a constant temperature of 85° C. A gas mixture consisting of N<sub>2</sub>/CO<sub>2</sub> (80:20) was constantly bubbled through the culture at a rate of 20 ml/min. The anaerobic growth medium consisted of a modified Allen's formulation (see below) (17) and was continuously added to the vessel at a rate of 8.0 ml/h using a Gilson Minipuls2 peristaltic pump (Gilson Inc., Middleton, WI, USA). Culture effluent was allowed to overflow through a side port in the cultivation vessel and into a sterile, anaerobic 2 l glass media bottle.

Obsidian Pool fermentor (OPF) medium (modified from Allen, 1959)

(NH <sub>4</sub> ) <sub>2</sub> SO <sub>4</sub>	1.30 g
KH <sub>2</sub> PO <sub>4</sub>	0.28 g
MgSO <sub>4</sub> x 7 H <sub>2</sub> O	0.25 g
CaSO <sub>4</sub> x 2 H <sub>2</sub> O	0.17 g
CaCl <sub>2</sub> x 2 H <sub>2</sub> O	0.07 g
FeCl <sub>3</sub> x 6 H <sub>2</sub> O	0.02 g
Na <sub>2</sub> SO <sub>4</sub>	0.07 g
KNO <sub>3</sub>	0.10 g
Peptone	0.50 g
Yeast Extract	0.10 g
Na <sub>2</sub> S <sub>2</sub> O <sub>3</sub>	0.78 g
Na <sub>2</sub> S x 6 H <sub>2</sub> O	0.13 g
MnCl <sub>2</sub> x 4 H <sub>2</sub> O (10 mg/ml)	180 µl
Na <sub>2</sub> B <sub>4</sub> O <sub>7</sub> x 10 H <sub>2</sub> O (25 mg/ml)	180 µl
ZnSO <sub>4</sub> x 7 H <sub>2</sub> O (10 mg/ml)	22 µl
CuCl <sub>2</sub> x 2 H <sub>2</sub> O (10 mg/ml)	5 µl
Na <sub>2</sub> MoO <sub>4</sub> x 2 H <sub>2</sub> O (1 mg/ml)	30 µl
VOSO <sub>4</sub> x 5 H <sub>2</sub> O (1 mg/ml)	30 µl
CoSO <sub>4</sub> x 7 H <sub>2</sub> O (1 mg/ml)	10 µl
LiCl/Na <sub>2</sub> WO <sub>4</sub> /NaSeO <sub>3</sub> /Ni(NH <sub>4</sub> ) <sub>2</sub> (SO <sub>4</sub> ) (1 mg/ml each)	10 µl
Wolfe's Vitamin Solution (1000X)	1.0 ml
Distilled H <sub>2</sub> O	1000 ml

**Fluorescent *In-situ* Hybridization Analysis.** Fresh samples were harvested directly from the Obsidian Pool enrichment culture and washed 3 times with 1 ml of phosphate buffered saline (PBS; pH 7.2). The cells were then spotted onto precleaned, gelatin coated microscope slides in 8 µl aliquots and dried by placing the slides onto a 50°C heat block. Ten microliters of fixative solution [3% paraformaldehyde (w/v) in PBS (pH 7.2)] was placed over the dried cells and the samples were then incubated either at RT for 2 h or overnight at 4°C. The fixed cells were washed thoroughly by rinsing the slides with PBS (pH 7.2) followed by an ethanol dehydration series by submerging the slides into a 50%, 70%, and 100% ethanol (v/v) bath for 3 min each. The slides

were then dried by applying a gentle stream of compressed air. A hybridization chamber was prepared by saturating a folded paper towel with hybridization buffer and placing the towel in a 50 ml conical centrifuge tube. A volume of 8  $\mu$ l of hybridization solution containing 0.9 M NaCl, 0.01%-0.5% (w/v) sodium dodecyl sulfate (SDS), 100  $\mu$ g/ml sheared herring sperm DNA, 0.02 M Tris-HCl (pH 7.2), and 0-40% formamide (v/v) were applied to each cell spot and the slides were placed in the hybridization chamber and incubated at 46°C for 15 min. After the prehybridization step, 100 ng of the appropriate fluorescently labeled, oligonucleotide probe was added to the hybridization buffer and the slides were incubated at 46°C for 3 h. Excess probe was washed from the slide by gently pipetting 2 ml pre-warmed wash buffer containing 0.9M-0.06 M NaCl (depending of formamide concentration in hybridization buffer), 0.1% (w/v) SDS, and 0.02 M Tris-Hcl (pH 7.2) over the cells. The entire slide was then immersed in pre-warmed wash buffer and placed in a 48°C water bath for 15 min. The slide was then rinsed with ca. 300 ml of deionized H<sub>2</sub>O and dried by applying a gentle stream of compressed air. A drop of Prolong Gold mounting solution containing 4',6-Diamidino-2-phenylindole (DAPI) (Molecular Probes, San Diego, CA, USA) was applied to each cell spot followed by a 25 x 25 mm coverslip. All microscopic analysis was performed with a Zeiss Axioplan 2 microscope (Jena, Germany) with 100 W mercury arc and halogen illumination sources. Phase contrast images were collected using either 63X, or 100X Plan Neofluar oil immersion objectives with 1.4 and 1.3 numerical apertures respectively. Images were collected using a Zeiss AxioCam digital camera and processed with Zeiss Axiovision software.

**Electron Microscopy.** *Korarchaeota* cell pellets were fixed in a solution containing 2.5% glutaraldehyde (EM grade) in 20 mM sodium cacodylate buffer (pH 6.5). For scanning electron microscopy drops of the fixed sample were placed onto glass slides, covered with a cover slip and rapidly frozen with liquid nitrogen. The cover slip was removed with a razor blade and the slide was immediately transferred into fixative buffer, postfixed with osmium tetroxide, dehydrated in a graded series of acetone solutions and critical-point dried from liquid CO<sub>2</sub>, mounted on stubs, and coated with 3 nm platinum with a magnetron sputter coater. The specimens were examined with a Hitachi S-4100 field emission scanning electron microscope. For negative staining a drop of the sample at appropriate dilution was placed on a 400 mesh carbon-coated copper grid, freshly hydrophilized by glow discharge. After incubation for 2 min, the drop was quickly removed with a pasteur pipette and the grid was air dried. The grid was stained with 2% uranium acetate and 0.01% glucose. Micrographs were taken with an EM 912 electron microscope (Zeiss) equipped with an integrated OMEGA energy filter operated in the zero loss mode.

**Cell Purification.** Culture effluent from the Obsidian Pool fermentor was collected anaerobically in sterile 2 l glass bottles. The cells were pelleted by centrifugation at 6000 rpm in a Beckman JLA-10.500 rotor for 20 min at 25°C in 500 ml centrifuge bottles (Nalgene, Rochester, NY, USA). The cells were resuspended in a total volume of 200 ml of PBS (pH 7.2) and then divided into 4 x 50 ml aliquots in 50 ml conical centrifuge tubes (BD Falcon, Bedford, MA, USA). The cells were centrifuged again at 6000 rpm for 20 min in a Beckman JA-12 rotor at 25°C and the supernatant was discarded. Each pellet was resuspended again in 50 ml of PBS (pH 7.2) by vortexing. After the cell pellets were completely resuspended, 0.5 ml of a 20% (w/v) SDS solution [final conc. 0.2% SDS (w/v)] was added to each tube and immediately mixed by inverting the tube several times. The tubes were centrifuged again at 6000 rpm for 20 min in a Beckman JA-12 rotor at 25°C. Each pellet was then washed 3 times by resuspending in 50 ml of PBS (pH 7.2) and centrifuging as



described above. After the final wash, the cell suspensions were heated to 85° C and then filtered through 0.45 µm syringe filters (MILLEX HV, Millipore, Carrigtwohill, Co. Cork, Ireland) in 25 ml aliquots. The filtrate was collected in fresh conical centrifuge tubes which were then centrifuged at 6000 rpm for 30 min in a Beckman JA-12 rotor at 4° C. Small white pellets were resuspended in a total volume of 1 ml of PBS (pH 7.2), placed in an Eppendorf tube, and centrifuged at 13,000 rpm in a benchtop microcentrifuge. The single cell pellet was resuspended in either PBS (pH 7.2) for microscopic analysis or DNA isolation.

**Genome Sequencing and Assembly.** Library construction, high-throughput sequencing, and genome assembly were performed at the Joint Genome Institute, Walnut Creek, CA, USA. Fosmid libraries were constructed from the raw OPF1 enrichment culture DNA and DNA from filtered cells using the pCC1FOS based system (Epicentre Biotechnologies, Madison, WI, USA). Small-insert libraries (2-3 kb insert size) were produced for raw, filtered, and purified cell samples of “*Ca. K. cryptofilum*”. DNA sequencing was performed with BigDye Terminators v3.1 and resolved with ABI PRISM 3730 DNA sequencers (PE Applied Biosystems, Foster City, CA, USA). The sequencing reads were base called using phred version 0.990722.g (18, 19), vector trimmed using crossmatch SPS-3.57, and assembled into contigs using parallel phrap ([www.phrap.org](http://www.phrap.org)). The contigs were aligned with an 84.7 kb “*Ca. K. cryptofilum*” genomic sequence containing the pOPF\_08 16S rRNA gene, and the 16S rRNA genes from *Thermofilum pendens* and *Thermosphaera aggregans*. The resulting assembly was binned by scaffolding and read depth, and by aligning binned scaffolds against the 16S rRNA sequences from the predominant archaeal genomes in the mixture and an 84.7 kb reference contig.

**Gene Prediction and Comparative Analysis.** An automated annotation was provided by the Computational Biology Group at Oak Ridge National Laboratory (ORNL), Oak Ridge, TN, USA. An additional analysis was performed by loading the complete korarchaeal genome into the Integrated Microbial Genomes (IMG) analysis tool developed by the Joint Genome Institute, Walnut Creek, CA, USA (20). To identify putative functions for the predicted open reading frames, the gene models were compared against all non-redundant (NR) sequences deposited in the National Center for Biotechnology Information (NCBI) database using BLASTP (21). The gene models were also compared against the protein families (Pfam) (22), Clusters of Orthologous Groups (COGs) (23), and the Kyoto Encyclopedia of Genes and Genomes (KEGG) (24) databases for further functional information. The BLAST E-value threshold was set at 1e-05. The Pfam threshold was also set at 1e-05. The COG search was performed using the default cutoff. For tRNA identification, tRNAscan-SE was run using the prokaryotic default settings (25), followed by manual analyses. DNA and amino acid sequence alignments were generated with CLUSTALW using the default parameters (26) and checked and edited manually using BioEdit v7.0.5 (<http://www.mbio.ncsu.edu/BioEdit/bioedit.html>).

**Phylogenetic Analyses.** An alignment of concatenated small and large subunit rRNA sequences (SSU+LSU rRNA) was constructed based on their conserved secondary structures and refined by hand using BioEdit (<http://www.mbio.ncsu.edu/BioEdit/bioedit.html>). Highly variable loop regions that could not be confidently aligned as well as regions in which some sequences were incomplete were masked out. The final alignment contained 27 taxa and 2965 nucleotide characters and was analyzed using the software Modeltest v3.7 to determine the best evolutionary

model that fits the data (27). The likelihood ratio test statistics indicated that to correspond to the general time reversible model with unequal nucleotide frequencies, a fraction of invariable sites and with six independent substitution rates that follow a gamma distribution (GTR+I+G). Phylogenetic analysis was performed using PAUP\* 4.0b8 (Sinauer Associates, Sunderland, MA). The initial GTR+I+G parameters were determined using five rounds of neighbor-joining tree construction/parameter estimation and were used for an unrestricted heuristic maximum likelihood tree search with random sequence addition and tree bisection-reconnection (TBR) branch swapping. The GTR+I+G parameters were estimated from the resulting tree and used for a new round of heuristic search that used five independent rounds of random sequence additions and TBR branch swapping, resulting in a single maximum likelihood tree. Bootstrapping (100 replicates) was conducted using the same parameters and one round of random sequence addition/TBR branch swapping for each replicate.

Protein sequences were aligned on the M-Coffee web server using a combination of multiple sequence alignment methods (28). The alignments were visually inspected and the regions not confidently aligned or containing high variability were masked out. The final alignments contained 476 aminoacid positions for EF2 and 211 aminoacid positions for FtsZ genes, respectively. Rooted (Fig. 2B) and unrooted (SI Fig. 8) EF2 trees were both calculated. Phylogenetic reconstruction was performed using two different approaches. First, the amino acid substitution model was chosen with the software Modelgenerator v84, which uses Akaike and Bayesian information criteria (AIC and BIC) to select the optimum among 88 different models (29). For all the datasets the optimum model was a combination of the RtRev substitution matrix with an estimated fraction of invariable sites and with six categories of substitution rates following a gamma distribution with the shape parameter optimized based on the data. These parameters were used to calculate maximum likelihood trees and non-parametric bootstrap support for the individual nodes with the PhyML v2.4.4 software (30). Since accurate reconstruction of deep phylogenetic branching order is complicated due to long branch attraction artifacts, we also used tree inference with PhyloBayes v2.3 (31). That software employs a Bayesian Monte Carlo Markov Chain (MCMC) sampler and a site-heterogeneous mixture model (CAT) and has been shown to be less prone to LBA (31, 32). Two to four independent chains were run in parallel for at least 10,000 generations starting from random trees, until convergence (maximum discrepancy across all bipartitions of <0.05). The first 5,000 cycles were then discarded as the burn-in and the remaining ones were sampled each of every ten to calculate majority-rule posterior consensus trees with bipartition frequencies at each node.

Concatenated r-protein and RNAP trees: Using the COGNITOR method (33, 34), representatives of three bacterial species (*E. coli*, *B. subtilis* and *D. radiodurans*) were added to the arCOGs that include 33 universally conserved ribosomal proteins and three largest RNA polymerase subunits. The sequences were aligned using MUSCLE (35). Start codon positions were verified and, when necessary, corrected manually. Maximum Likelihood trees for the concatenated alignment of 36 proteins (8057 aminoacid positions, 5696 for ribosomal proteins and 2361 for RNA polymerase subunits) were constructed using TreeFinder (14), with the Whelan and Goldman (WAG) evolutionary model and gamma-distributed site rates. Tree topologies were compared using the Approximately Unbiased test (AU) (13) implemented in the TreeFinder program. The topology

where “*Ca. K. cryptofilum*” is a sister group of all Crenarchaeota, including *Cenarchaeum symbiosum* passed the 0.05 p-value cut-off (AU p-value = 0.17).

### Supplementary References:

1. Burggraf S, Huber H, Stetter KO (1997) Reclassification of the crenarchael orders and families in accordance with 16S rRNA sequence data. *Int J Syst Bacteriol* 47:657-660.
2. Spear JR, Walker JJ, McCollom TM, Pace NR (2005) Hydrogen and bioenergetics in the Yellowstone geothermal ecosystem. *Proc Natl Acad Sci U S A* 102:2555-2560.
3. Barns SM, Fundyga RE, Jeffries MW, Pace NR (1994) Remarkable archaeal diversity detected in a Yellowstone National Park hot spring environment. *Proc Natl Acad Sci U S A* 91:1609-1613.
4. Reysenbach AL, Ehringer M, Hershberger K (2000) Microbial diversity at 83 degrees C in Calcite Springs, Yellowstone National Park: another environment where the Aquificales and "Korarchaeota" coexist. *Extremophiles* 4:61-67.
5. Raskin L, Stromley JM, Rittmann BE, Stahl DA (1994) Group-specific 16S rRNA hybridization probes to describe natural communities of methanogens. *Appl Environ Microbiol* 60:1232-1240.
6. Amann RI, Binder BJ, Olson RJ, Chisholm SW, Devereux R, Stahl DA (1990) Combination of 16S rRNA-targeted oligonucleotide probes with flow cytometry for analyzing mixed microbial populations. *Appl Environ Microbiol* 56:1919-1925.
7. Nishida H, Nishiyama M, Kobashi N, Kosuge T, Hoshino T, Yamane H (1999) A prokaryotic gene cluster involved in synthesis of lysine through the amino adipate pathway: a key to the evolution of amino acid biosynthesis. *Genome Research* 9:1175-1183.
8. White RH (2004) L-Aspartate semialdehyde and a 6-deoxy-5-ketohexose 1-phosphate are the precursors to the aromatic amino acids in *Methanocaldococcus jannaschii*. *Biochemistry* 43:7618-7627.
9. Mahillon J, Chandler M (1998) Insertion sequences. *Microbiol Mol Biol Rev* 62:725-774.
10. Filee J, Siguier P, Chandler M (2007) Insertion sequence diversity in archaea. *Microbiol Mol Biol Rev* 71:121-157.
11. She Q, Singh RK, Confalonieri F, Zivanovic Y, Allard G, Awayez MJ, Chan-Weiher CC, Clausen IG, Curtis BA, De Moors A, Erauso G, Fletcher C, Gordon PM, Heikamp-de Jong I, Jeffries AC, Kozera CJ, Medina N, Peng X, Thi-Ngoc HP, Redder P, Schenk ME, Theriault C, Tolstrup N, Charlebois RL, Doolittle WF, Duguet M, Gaasterland T, Garrett RA, Ragan MA, Sensen CW, Van der Oost J (2001) The complete genome of the crenarchaeon *Sulfolobus solfataricus* P2. *Proc Natl Acad Sci U S A* 98:7835-7840.
12. Greve B, Jensen S, Brugger K, Zillig W, Garrett RA (2004) Genomic comparison of archaeal conjugative plasmids from *Sulfolobus*. *Archaea* 1:231-239.
13. Shimodaira H (2002) An approximately unbiased test of phylogenetic tree selection. *Syst Biol* 51:492-508.
14. Jobb G, von Haeseler A, Strimmer K (2004) TREEFINDER: a powerful graphical analysis environment for molecular phylogenetics. *BMC Evol Biol* 4:18.
15. Brochier C, Forterre P, Gribaldo S (2004) Archaeal phylogeny based on proteins of the transcription and translation machineries: tackling the *Methanopyrus kandleri* paradox. *Genome Biol* 5:R17.

16. Shock EL, Holland M, Meyer-Dombard D, Amend JP (2005) in *Geothermal Biology and Geochemistry in Yellowstone National Park*, ed. Inskeep WP (Thermal Biology Institute, Montana State University, Bozeman), pp. 95-112.
17. Allen MB (1959) Studies with *Cyanidium caldarium*, an anomalously pigmented chlorophyte. *Arch Mikrobiol* 32:270-277.
18. Ewing B, Green P (1998) Base-calling of automated sequencer traces using phred. II. Error probabilities. *Genome Res* 8:186-194.
19. Ewing B, Hillier L, Wendl MC, Green P (1998) Base-calling of automated sequencer traces using phred. I. Accuracy assessment. *Genome Res* 8:175-185.
20. Markowitz VM, Korzeniewski F, Palaniappan K, Szeto E, Werner G, Padki A, Zhao X, Dubchak I, Hugenholtz P, Anderson I, Lykidis A, Mavromatis K, Ivanova N, Kyrpides NC (2006) The integrated microbial genomes (IMG) system. *Nucleic Acids Res* 34:D344-348.
21. Altschul SF, Madden TL, Schaffer AA, Zhang J, Zhang Z, Miller W, Lipman DJ (1997) Gapped BLAST and PSI-BLAST: a new generation of protein database search programs. *Nucleic Acids Res* 25:3389-3402.
22. Finn RD, Mistry J, Schuster-Bockler B, Griffiths-Jones S, Hollich V, Lassmann T, Moxon S, Marshall M, Khanna A, Durbin R, Eddy SR, Sonnhammer EL, Bateman A (2006) Pfam: clans, web tools and services. *Nucleic Acids Res* 34:D247-251.
23. Tatusov RL, Galperin MY, Natale DA, Koonin EV (2000) The COG database: a tool for genome-scale analysis of protein functions and evolution. *Nucleic Acids Res* 28:33-36.
24. Kanehisa M, Goto S, Hattori M, Aoki-Kinoshita KF, Itoh M, Kawashima S, Katayama T, Araki M, Hirakawa M (2006) From genomics to chemical genomics: new developments in KEGG. *Nucleic Acids Res* 34:D354-357.
25. Lowe TM, Eddy SR (1997) tRNAscan-SE: a program for improved detection of transfer RNA genes in genomic sequence. *Nucleic Acids Res* 25:955-964.
26. Chenna R, Sugawara H, Koike T, Lopez R, Gibson TJ, Higgins DG, Thompson JD (2003) Multiple sequence alignment with the Clustal series of programs. *Nucleic Acids Res* 31:3497-3500.
27. Posada D, Crandall KA (1998) MODELTEST: testing the model of DNA substitution. *Bioinformatics* 14:817-818.
28. Moretti S, Armougom F, Wallace IM, Higgins DG, Jongeneel CV, Notredame C (2007) The M-Coffee web server: a meta-method for computing multiple sequence alignments by combining alternative alignment methods. *Nucleic Acids Res* 35:W645-648.
29. Keane TM, Creevey CJ, Pentony MM, Naughton TJ, McLnerney JO (2006) Assessment of methods for amino acid matrix selection and their use on empirical data shows that ad hoc assumptions for choice of matrix are not justified. *BMC Evol Biol* 6:29.
30. Guindon S, Gascuel O (2003) A simple, fast, and accurate algorithm to estimate large phylogenies by maximum likelihood. *Syst Biol* 52:696-704.
31. Lartillot N, Brinkmann H, Philippe H (2007) Suppression of long-branch attraction artefacts in the animal phylogeny using a site-heterogeneous model. *BMC Evol Biol* 7 Suppl 1:S4.
32. Philippe H, Brinkmann H, Martinez P, Riutort M, Baguna J (2007) Acoel flatworms are not platyhelminthes: evidence from phylogenomics. *PLoS ONE* 2:e717.
33. Tatusov RL, Koonin EV, Lipman DJ (1997) A genomic perspective on protein families. *Science* 278:631-637.

34. Makarova KS, Sorokin AV, Novichkov PS, Wolf YI, Koonin EV (2007) Clusters of orthologous genes for 41 archaeal genomes and implications for evolutionary genomics of archaea. *Biol Direct* 2:33.
35. Edgar RC (2004) MUSCLE: multiple sequence alignment with high accuracy and high throughput. *Nucleic Acids Res* 32:1792-1797.
36. Brunk CF, Eis N (1998) Quantitative measure of small-subunit rRNA gene sequences of the kingdom korarchaeota. *Appl Environ Microbiol* 64:5064-5066.
37. Baker GC, Smith JJ, Cowan DA (2003) Review and re-analysis of domain-specific 16S primers. *J Microbiol Methods* 55:541-555.

### Supporting Figure Legends:

**Fig. 3.** Neighbour-Joining tree constructed from distance matrix analysis of SSU rDNA sequences obtained from the Obsidian Pool enrichment culture. “*Ca. K. cryptofilum*” is represented by clone pOPF\_08.

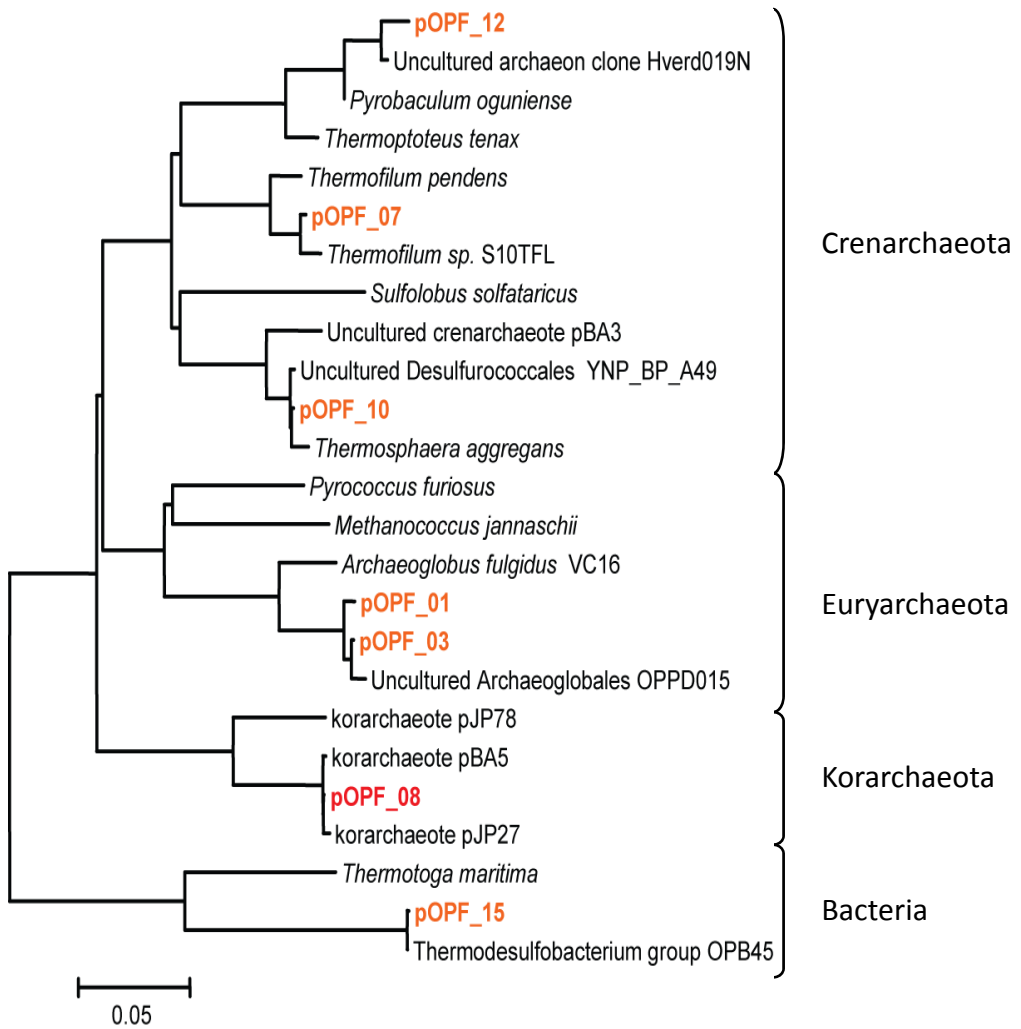
**Fig. 4.** Fluorescence *in-situ* hybridization analysis using crenarchaeal and *Korarchaeota* specific probes. (A) Pure culture of *Thermofilum* sp. S10TFL hybridizing to Alexa488-labeled CREN499R (CCARNCTTGCCCCCGCT) probe. (B) CREN499R probe applied to Obsidian Pool enrichment culture. (C) Cy3-labeled *Korarchaeota* specific probes KR515R (CCAGCCTTACCCTCCCCT) and KR565R (AGTATGCGTGGGAACCCCTC) hybridizing to cells of “*Ca. K. cryptofilum*”. (D) Phase contrast image of cell preparation. Scale bars represent 5µm.

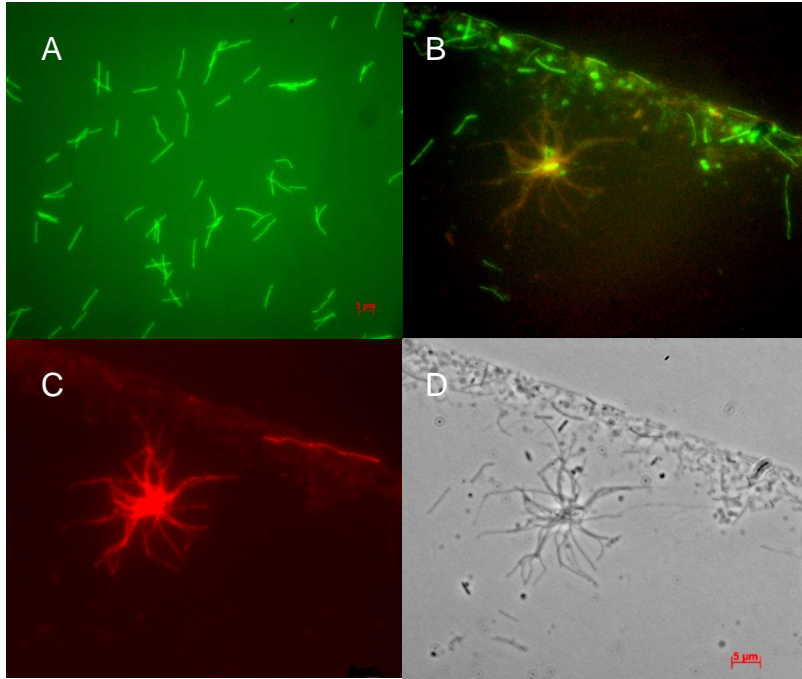
**Fig. 5.** Relative abundance of PCR amplified SSU rDNAs obtained from (A), untreated, Obsidian Pool enrichment culture and (B), filtered cells exposed to 0.2% SDS for 15 min. PCR primers included Ab779F (GCRAASSGGATTAGATACCC) (36) and UA1406R (ACGGGCGGTGWGTRCAA) (37). The treatment resulted in a highly enriched cell fraction of cells represented by the pOPF\_08 SSU rDNA sequence type.

**Fig. 6.** Prior to WGS sequencing, fosmid clones containing the pOPF\_08 SSU rRNA sequence were retrieved and assembled from a library constructed from Obsidian Pool enrichment culture DNA with a CopyControl fosmid library kit (Epicentre, Madison, WI, USA). (A) Fosmid clone pKOR01M18 containing korarchaeal small and large subunit rRNA genes was retrieved by probing the library with a 209 bp, 5' region of the pOPF\_08 sequence. The LSU rRNA gene contains a self splicing, intron- encoded LAGLIDADG type endonuclease. (B) Additional clones were retrieved by probing the library with labelled end-sequences from the finished fosmids. Overlapping fosmid clones were assembled to construct an 84.7 kb genomic contig.

**Fig. 7.** Majority-rule posterior consensus tree (PhyloBayes) for FtsZ protein sequences. Values at the nodes indicate the posterior probability for that branching (the branch was collapsed when the value was <50). Scale bar indicates the inferred number of substitutions per site.

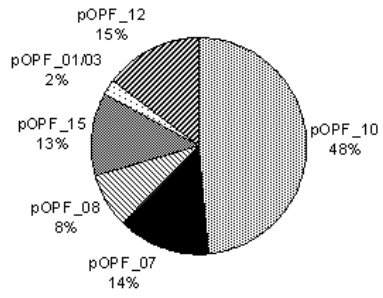
**Fig. 8.** Unrooted archaeal phylogeny based on translation elongation factor 2 (EF2) proteins. The numbers indicate bootstrap support for PhyML/consensus posterior probability (Phyloblast), an asterisk indicates <50 bootstrap support. Where both values were <50, the branch was collapsed. Scale bar indicates the inferred number of substitutions per site.





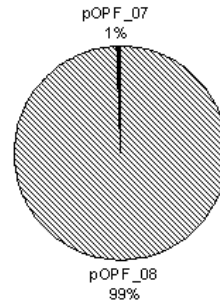


A.

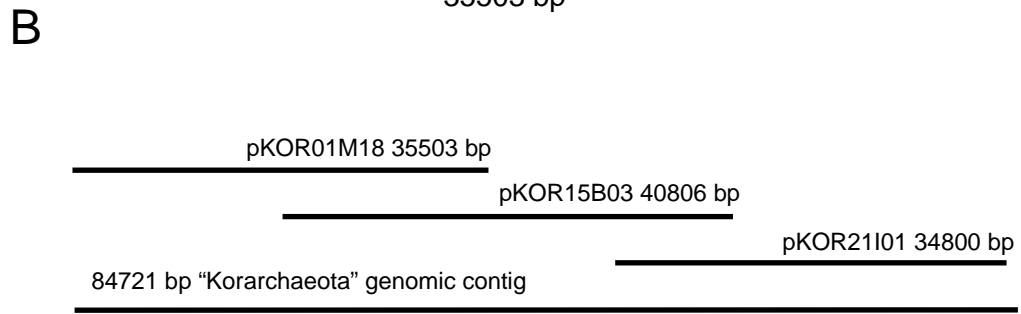
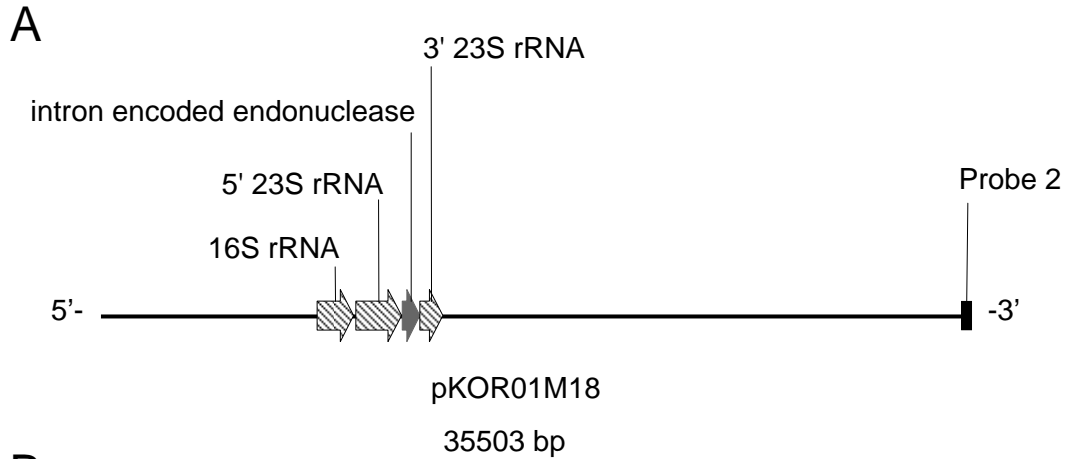


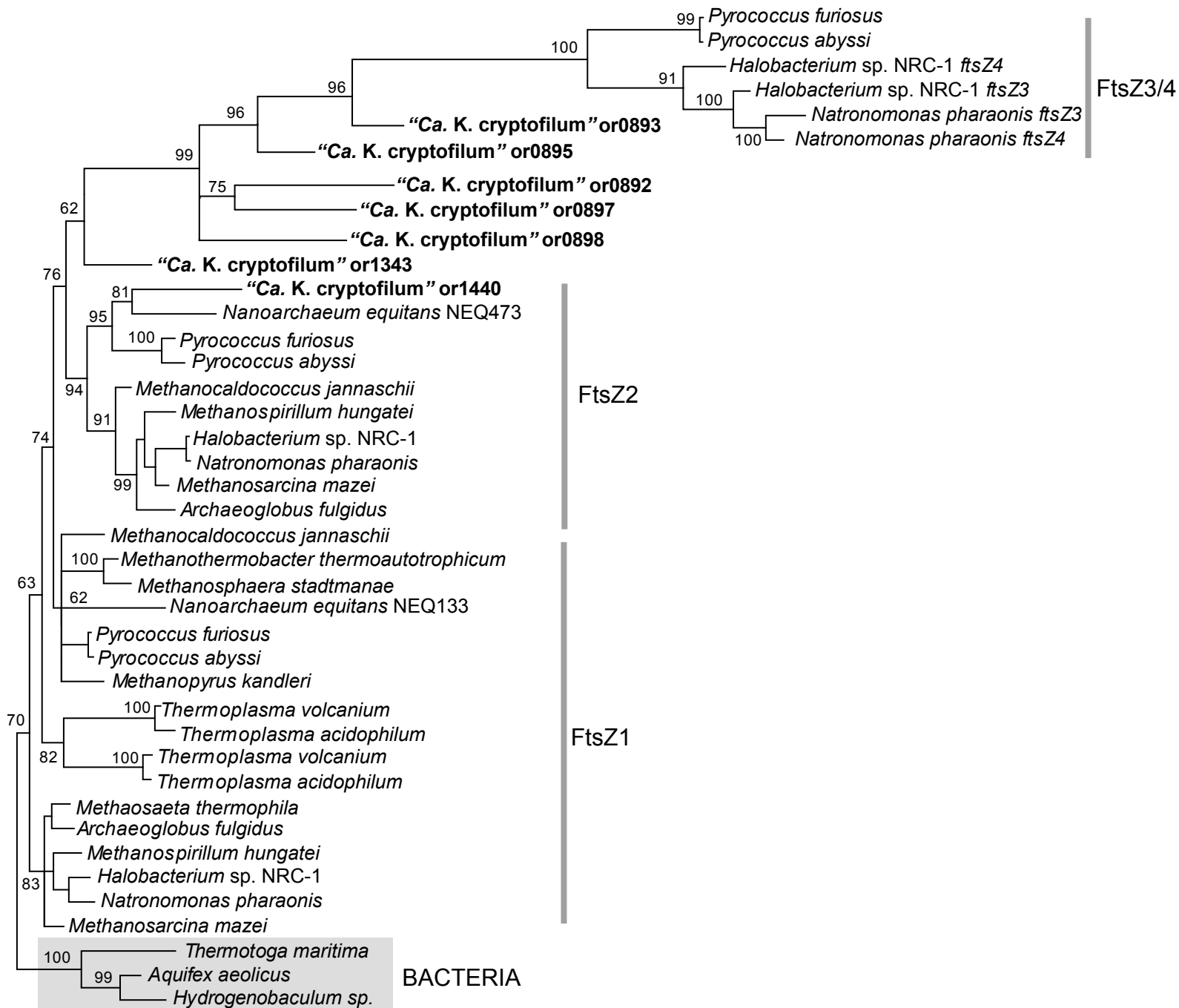
N=176

B.



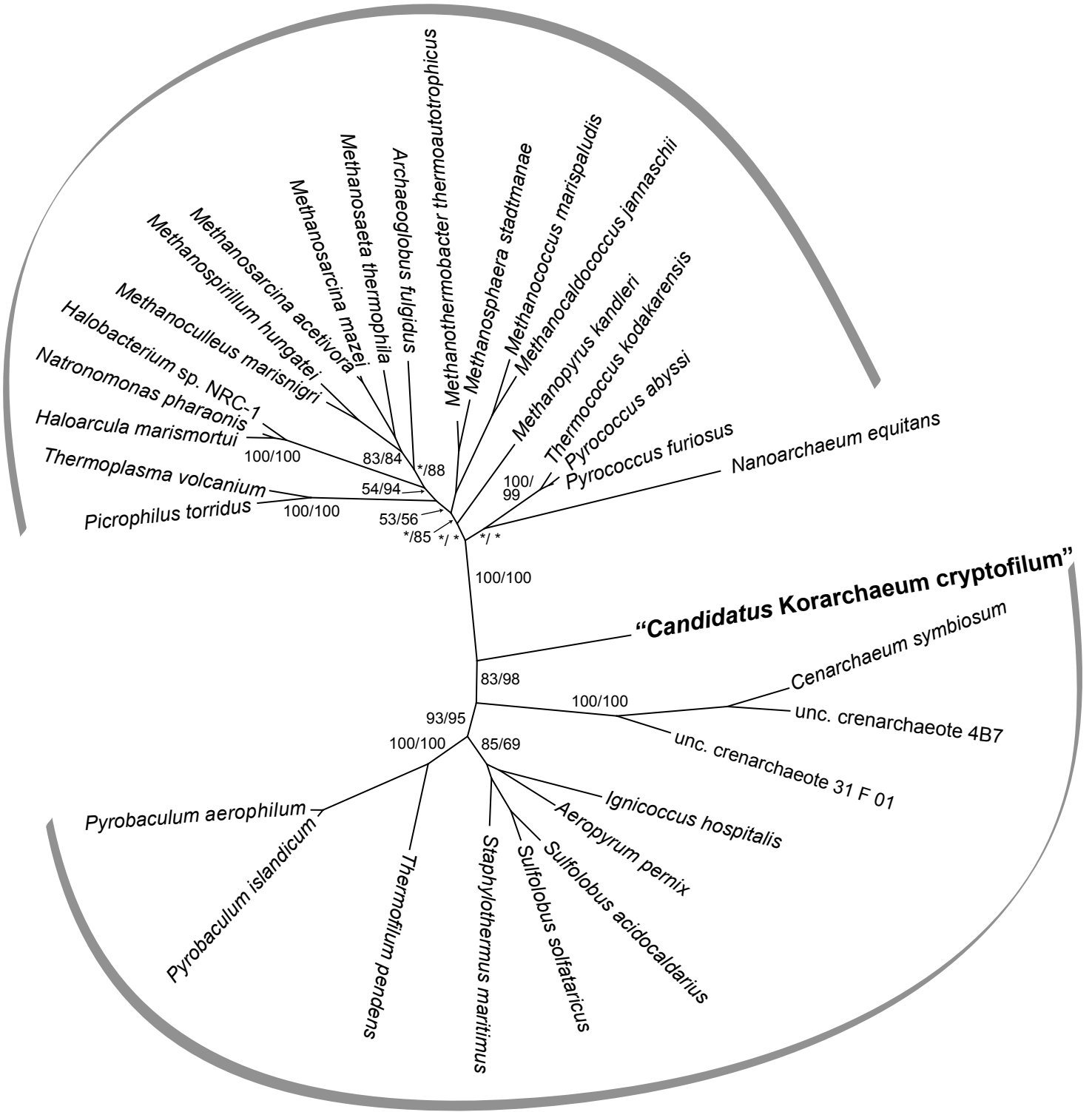
N=180





0.2

# Euryarchaeota







































Gene	Strand	Start	Stop	Size (a.a.)	Product	Gene Name	COGs	arCOGs	COG_gene	Func	arCOG annotation	# of Cren in arCOGs	#
Kcr_1573	+	1552439	1553842	468	SecY protein			arCOG04169	SecY	U	Preprotein translocase subunit SecY	13	2
Kcr_1574	+	1553847	1554350	168	membrane protein-like			arCOG02673	-	S	Predicted membrane protein	1	2
Kcr_1575	+	1554465	1554764	100	Ribosomal protein L34e			arCOG04168	RPL34A	J	Ribosomal protein L34E	11	1
Kcr_1576	+	1554800	1555078	93	ribosomal protein L14E			arCOG04167	RPL14A	J	Ribosomal protein L14E/L6E/L27E	12	1
Kcr_1577	+	1555075	1556052	326	Pseudouridylylase			arCOG00987	TruB	J	Pseudouridine synthase	13	2
Kcr_1578	+	1556459	1556908	150	ribosomal protein S13		rrsD	arCOG01722	RpsM	J	Ribosomal protein S13	13	2
Kcr_1579	+	1556918	1557418	167	ribosomal protein S4			arCOG04239	RpsD	J	Ribosomal protein S4 or related protein	13	2
Kcr_1580	+	1557418	1557816	133	ribosomal protein S11			arCOG04240	RpsK	J	Ribosomal protein S11	13	2
Kcr_1581	+	1557882	1558820	313	hypothetical protein								
Kcr_1582	+	1558801	1559556	252	RNA polymerase, insert			arCOG04241	RpoA	K	DNA-directed RNA polymerase subunit D	13	2
Kcr_1583	-	1559705	1560853	383	Cytochrome bd-type quinol oxidase subunit 1-like			arCOG02720	CydA	C	Cytochrome bd-type quinol oxidase, subunit 1	5	1
Kcr_1584	-	1560856	1562472	539	cytochrome bd ubiquinol oxidase, subunit I			arCOG02721/3	CydA	C	Cytochrome bd-type quinol oxidase, subunit 1	5	7
Kcr_1585	+	1562730	1564031	434	major facilitator superfamily MFS_1			arCOG02682	ProP	G	permease of the major facilitator superfamily	10	5
Kcr_1586	+	1564149	1564511	121	ribosomal protein L15			arCOG00780	RPL18A	J	Ribosomal protein L18E	13	2
Kcr_1587	+	1564517	1564993	159	ribosomal protein L13	L13		arCOG04242	RplM	J	Ribosomal protein L13	13	2
Kcr_1588	+	1564977	1565396	140	ribosomal protein S9			arCOG04243	RpsI	J	Ribosomal protein S9	13	2
Kcr_1589	+	1565423	1565827	135	translation initiation factor eIF-5A	eIF_5A		arCOG04277	Efp	J	Translation elongation factor P (EF-P)/translation initiation factor 5A (eIF-5A)	13	2
Kcr_1590	+	1565832	1567145	438	GTP-binding signal recognition particle SRP54, G-domain			arCOG01228	Ffh	U	Signal recognition particle GTPase	13	2
Kcr_1591	+	1567189	1568310	374	conserved hypothetical protein			arCOG01015	-	J	Predicted pseudouridylylase	13	2
Kcr_1592	+	1568325	1568621	99	ribosomal protein L21e			arCOG04129	RPL21A	J	Ribosomal protein L21E	13	2
Kcr_1593	+	1568624	1568980	119	RNA polymerase Rpb4			arCOG01016	-	K	DNA-directed RNA polymerase, subunit F (rpoF)	13	2
Kcr_1594	+	1569001	1569576	192	putative nucleotide binding protein			arCOG04130	-	J	Predicted RNA-binding protein	13	2
Kcr_1595	-	1569569	1570303	245	aspartate/glutamate/uridylylase kinase			arCOG00860	-	R	Predicted archaeal kinase	11	2
Kcr_1596	+	1570353	1571942	530	ATPase			arCOG04116	-	R	ATPase (PIT family)	13	2
Kcr_1597	-	1571921	1572460	180	Cytidylyltransferase-related			arCOG00972	NadR	H	Nicotinamide mononucleotide adenylyltransferase	13	2
Kcr_1598	-	1572555	1573247	231	NUDIX hydrolase			arCOG01075/1	-	F	NUDIX family hydrolase	12	2
Kcr_1599	-	1573247	1574104	286	ATPase, BadF/BadG/BcrA/BcrD type			arCOG02679/2	-	I	Activator of 2-hydroxyglutaryl-CoA dehydratase (HSP70-class ATPase domain)	0	1
Kcr_1600	-	1574101	1574652	184	hypothetical protein								
Kcr_1601	-	1574669	1575298	210	metallophosphoesterase			arCOG01145	-	R	lcc family phosphoesterase	11	2
Kcr_1602	+	1575350	1576354	335	Radical SAM			arCOG00951	-	R	Predicted Fe-S oxidoreductase	9	1
Kcr_1603	+	1576412	1577896	495	phenylalanyl-tRNA synthetase, alpha subunit	pheS		arCOG00410	PheS	J	Phenylalanyl-tRNA synthetase alpha subunit	13	2
Kcr_1604	+	1577901	1579571	557	phenylalanyl-tRNA synthetase, beta subunit	pheTa		arCOG00412	PheT	J	Phenylalanyl-tRNA synthetase beta subunit	13	2
Kcr_1605	-	1579688	1580731	348	peptidase M42			arCOG01518	FrvX	G	Cellulase M or related protein	9	2
Kcr_1606	+	1580785	1582050	422	Phosphopyruvate hydratase			arCOG01169	Eno	G	Enolase	13	2
Kcr_1607	-	1582028	1583419	464	tRNA adenylyltransferase			arCOG04249	CCA1	J	tRNA nucleotidyltransferase (CCA-adding enzyme)	13	2
Kcr_1608	-	1583403	1584008	202	sugar isomerase (SIS)			arCOG00068	GutQ	M	Predicted sugar phosphate isomerase involved in capsule formation	12	1
Kcr_1609	+	1584057	1584704	216	protein of unknown function DUF125, transmembrane			arCOG01091	-	S	Uncharacterized membrane protein	10	1
Kcr_1610	+	1584689	1585387	233	tRNA pseudouridylylase			arCOG04449	TruA	J	Pseudouridylylase	4	2
Kcr_1611	-	1585365	1585643	93	hypothetical protein								
Kcr_1612	-	1585742	1587238	499	Radical SAM			arCOG01355	-	C	Radical SAM superfamily enzyme	7	8
Kcr_1613	-	1587423	1588211	263	conserved hypothetical protein			arCOG04612	-	S	Uncharacterized protein conserved in archaea	0	1
Kcr_1614	-	1588208	1588738	177	Transcription factor TFIIe, alpha subunit			arCOG04270	TFA1	K	Transcription initiation factor IIe, alpha subunit	13	2
Kcr_1615	-	1589289	1589804	172	histidine triad (HIT) protein			arCOG00419	Hit	F	HIT family hydrolase	13	2
Kcr_1616	-	1589801	1590151	117	Alpha-NAC-related protein			arCOG04061	EGD2	K	Transcription factor homologous to NACalpha-BTF3	12	2
Kcr_1617	+	1590211	1590750	180	helix-turn-helix motif			arCOG01863	-	K	Predicted transcription factor, homolog of eukaryotic MBF1	12	2

**Table 4. Representation of genes that are characteristic of *Crenarchaeota* or *Euryarchaeota* in. “*Candidatus K. cryptofilum*”**

Locus Tag	arCOG	Functional class	Annotation	#Cren genomes	#Eury genomes
<b>Genes characteristic of <i>Euryarchaeota</i><sup>a</sup></b>					
<b>Kcr_1527</b>	<b>arCOG04447</b>	<b>Replication/repair</b>	<b>Archaeal DNA polymerase II, large subunit</b>	<b>0</b>	<b>27</b>
<b>Kcr_1385</b>	<b>arCOG04455</b>	<b>Replication/repair</b>	<b>Archaeal DNA polymerase II, small subunit</b>	<b>0</b>	<b>26</b>
<b>Kcr_1284</b>	<b>arCOG00872</b>	<b>Replication/repair</b>	<b>ERCC4-like helicase</b>	<b>0</b>	<b>26</b>
<b>Kcr_0242</b>	<b>arCOG02610</b>	<b>Replication/repair</b>	<b>Rec8/ScpA/Sccl-like protein (kleisin family)</b>	<b>0</b>	<b>24</b>
<b>Kcr_1446</b>	<b>arCOG02258</b>	<b>Replication/repair</b>	<b>RPA family protein, a subunit of RPA complex</b>	<b>0</b>	<b>20</b>
<b>Kcr_0892, 0893, 0895, 0897, 0898, 1343, 1440</b>	<b>arCOG02201</b>	<b>Cell division</b>	<b>Cell division GTPase FtsZ</b>	<b>0</b>	<b>26</b>
<b>Kcr_0243</b>	<b>arCOG00371</b>	<b>Cell division</b>	<b>Chromosome segregation ATPase, Smc</b>	<b>0</b>	<b>24</b>
Kcr_0227	arCOG01684	transcription	Predicted transcriptional regulator	0	22
Kcr_1298	arCOG03363	Energy metabolism	Archaeal/vacuolar-type H <sup>+</sup> -ATPase subunit H	0	26
Kcr_0321, 1119	arCOG01549	Energy metabolism	Coenzyme F420-reducing hydrogenase, alpha subunit	0	18
Kcr_1264	arCOG00959	Energy metabolism	Ferredoxin	0	18
Kcr_1262	arCOG01607	Energy metabolism	Pyruvate:ferredoxin oxidoreductase or related 2-oxoacid:ferredoxin oxidoreductase, alpha subunit	0	19
Kcr_1100	arCOG04353	Amino acid metabolism	3-dehydroquinase synthase	0	20
Kcr_0835	arCOG02714	Coenzyme metabolism	GTP and metal dependent enzyme involved F420 coenzyme biosynthesis	0	20
Kcr_0481	arCOG00043	General functional prediction only	ATP-utilizing enzyme of the PP-loop superfamily	0	18
Kcr_1356	arCOG00354	General functional prediction only	GTPase SAR1 or related small G protein	0	23
Kcr_0479	arCOG02465	General functional prediction only	NCAIR mutase (PurE)-related protein	0	18
Kcr_0896, 1002	arCOG02155	General functional prediction only	Protein implicated in RNA metabolism, contains PRC-barrel domain	0	26
Kcr_1574	arCOG02673	Uncharacterized	Predicted membrane protein	0	27
Kcr_1412	arCOG02263	Uncharacterized	Uncharacterized conserved protein	0	24
Kcr_1416	arCOG02197	Uncharacterized	Uncharacterized conserved protein	0	23
Kcr_1046	arCOG02408	Uncharacterized	Uncharacterized conserved protein	0	20
Kcr_0480	arCOG02701	Uncharacterized	Uncharacterized conserved protein	0	18
Missing in <i>K. cryptofilum</i> : 47 euryarchaeal-specific genes					
<b>Genes characteristic of <i>Crenarchaeota</i><sup>b</sup></b>					
<b>Kcr_0816</b>	<b>arCOG01013</b>	<b>Translation</b>	<b>Protein containing a domain similar to ribosomal protein L13E</b>	<b>11</b>	<b>0</b>
<b>Kcr_0040</b>	<b>arCOG04327</b>	<b>Translation</b>	<b>Ribosomal protein S25</b>	<b>13</b>	<b>0</b>
<b>Kcr_1513</b>	<b>arCOG04293</b>	<b>Translation</b>	<b>Ribosomal protein S30</b>	<b>13</b>	<b>0</b>
<b>Kcr_1196</b>	<b>arCOG04305</b>	<b>Translation</b>	<b>Ribosomal protein S26</b>	<b>13</b>	<b>0</b>
<b>Kcr_1004</b>	<b>arCOG04271</b>	<b>Transcription</b>	<b>DNA-directed RNA polymerase, subunit RPB8</b>	<b>12</b>	<b>0</b>
<b>Kcr_0112</b>	<b>arCOG00393</b>	<b>Transcription</b>	<b>Predicted membrane-associated transcriptional regulator</b>	<b>9</b>	<b>0</b>
Kcr_0586	arCOG00287	Replication/repair	Predicted NurA-like nuclease	10	0
Kcr_0394	arCOG02299	Secretion/motility	Peptidase A24A, prepilin type IV	12	0
Kcr_0105	arCOG02960	General functional prediction only	Predicted aminopeptidase, lap family	10	0
Kcr_1526	arCOG04136	General functional prediction only	Uncharacterized Zn ribbon-containing protein	12	0
Kcr_0281, 0620	arCOG01618	General functional prediction only	Aldo/keto reductase, related to diketogulonate reductase	9	0
Kcr_0852	arCOG03721	General functional prediction only	HEPN domain	10	0
Kcr_0392, 0733, 0851	arCOG03722	General functional prediction only	HEPN domain	9	0
Kcr_0387	arCOG03119	Uncharacterized	DedA family membrane protein	13	0
Kcr_1152	arCOG03770	Uncharacterized	Uncharacterized conserved protein	11	0
Missing in <i>K. cryptofilum</i> : 30 crenarchaeal-specific genes					

<sup>a</sup>Bold type shows genes for replication/repair and cell division system components

<sup>b</sup>Bold type shows genes for translation and transcription system components

**Table 5. Bacterial COGs without archaeal members except “*Ca. K. cryptofilum*”**

Locus Tag	COG	Function	Top BLASTP Hit	Accession #	E-value
Kcr_0172	COG0386	Glutathione peroxidase	<i>Desulfuromonas acetoxidans</i> DSM 684	ZP_01311479	7.0e-06
Kcr_0823	COG0861	Membrane protein TerC possibly involved in tellurium resistance	<i>Saccharopolyspora erythraea</i> NRRL 2338	YP_001105852	2.0e-59
Kcr_1396	COG1349	Transcriptional regulators of sugar metabolism	<i>Anaeromyxobacter dehalogenans</i> 2CP-1	ZP_02325805	6.7e-02
Kcr_0831	COG1760	L-serine deaminase	<i>Algoriphagus</i> sp. PR1	ZP_01720767	8.0e-70
Kcr_1493	COG1995	Pyridoxal phosphate biosynthesis protein	<i>Acidiphilium cryptum</i> JF-5	YP_001234273	1.0e-73
Kcr_1494	COG3395	Uncharacterized protein conserved in bacteria	<i>Alkaliphilus metalliredigens</i> QYMF	YP_001318120	5.0e-24
Kcr_1364	COG3485	Protocatechuate 3 4-dioxygenase beta subunit	<i>Desulfococcus oleovorans</i> Hxd3	YP_001530052	5.0e-06

**Table 6. Top BLASTP hits for predicted euryarchaeal specific genes in “*Ca. K. cryptofilum*”**

<b>Locus Tag</b>	<b>Function</b>	<b>Top BLASTP Hit</b>	<b>Accession #</b>	<b>E-value</b>
Kcr_0047	Histones H3 and H4	<i>Methanobacterium formicicum</i>	P48783	9.0e-14
Kcr_1137	Histones H3 and H4	<i>Thermococcus zilligii</i>	P95669	6.0e-14
Kcr_1527	Archaeal DNA polymerase II, large subunit	<i>Methanosaeta thermophila</i> PT	YP_843669	0.0
Kcr_1385	Archaeal DNA polymerase II, small subunit	<i>Methanosaeta thermophila</i> PT	YP_843089	1.0e-73
Kcr_1440	Cell division GTPase	<i>Thermococcus kodakarensis</i> KOD1	YP_184684	3.0e-68
Kcr_1343	Cell division GTPase	<i>Methanothermobacter thermautotrophicus</i> str. Delta H	NP_276787	1.0e-89
Kcr_0892	Cell division GTPase	<i>Thermococcus kodakarensis</i> KOD1	YP_184684	2.0e-38
Kcr_0893	Cell division GTPase	<i>Pyrococcus horikoshii</i> OT3	NP_142027	1.0e-28
Kcr_0895	Cell division GTPase	<i>Thermococcus kodakarensis</i> KOD1	YP_183834	2.0e-41
Kcr_0897	Cell division GTPase	<i>Pyrococcus abyssi</i> GE5	NP_126968	7.0e-29
Kcr_0898	Cell division GTPase	<i>Pyrococcus furiosus</i> DSM 3638	NP_578254	3.0e-42